Ca^{2+}-Dependent Excitation-Contraction Coupling Triggered by the Heterologous Cardiac/Brain DHPR β2a-Subunit in Skeletal Myotubes

David C. Sheridan, Leah Carbonneau, Chris A. Ahern, Priya Nataraj, and Roberto Coronado

Department of Physiology, University of Wisconsin, School of Medicine, Madison, Wisconsin 53706 USA

ABSTRACT   Molecular determinants essential for skeletal-type excitation-contraction (EC) coupling have been described in the cytosolic loops of the dihydropyridine receptor (DHPR) α1S pore subunit and in the carboxyl terminus of the skeletal-specific DHPR β1a-subunit. It is unknown whether EC coupling domains present in the β-subunit influence those present in the pore subunit or if they act independent of each other. To address this question, we investigated the EC coupling signal that is generated when the endogenous DHPR pore subunit α1S is paired with the heterologous heart/brain DHPR β2a-subunit. Studies were conducted in primary cultured myotubes from β1 knockout (KO), ryanodine receptor type 1 (RyR1) KO, ryanodine receptor type 3 (RyR3) KO, and double RyR1/RyR3 KO mice under voltage clamp with simultaneous monitoring of confocal fluo-4 fluorescence. The β2a-mediated Ca^{2+} current recovered in β1 KO myotubes lacking the endogenous DHPR β1a-subunit verified formation of the α1S/β1a pair. In myotube genotypes which express no or low-density L-type Ca^{2+} currents, namely β1 KO and RyR1 KO, β2a overexpression recovered a wild-type density of nifedipine-sensitive Ca^{2+} currents with a slow activation kinetics typical of skeletal myotubes. Concurrent with Ca^{2+} current recovery, there was a drastic reduction of voltage–dependent, skeletal-type EC coupling and emergence of Ca^{2+} transients triggered by the Ca^{2+} current. A comparison of β2a overexpression in RyR3 KO, RyR1 KO, and double RyR1/RyR3 KO myotubes concluded that both RyR1 and RyR3 isoforms participated in Ca^{2+}-dependent Ca^{2+} release triggered by the β2a-subunit. In β1 KO and RyR1 KO myotubes, the Ca^{2+}-dependent EC coupling promoted by β2a overexpression had the following characteristics: 1), L-type Ca^{2+} currents had a wild-type density; 2), Ca^{2+} transients activated much slower than controls overexpressing β1a, and the rate of fluorescence increase was consistent with the activation kinetics of the Ca^{2+} current; 3), the voltage dependence of the Ca^{2+} transient was bell-shaped and the maximum was centered at $\sim$+30 mV, consistent with the voltage dependence of the Ca^{2+} current; and 4), Ca^{2+} currents and Ca^{2+} transients were fully blocked by nifedipine. The loss in voltage-dependent EC coupling promoted by β2a was inferred by the drastic reduction in maximal Ca^{2+} fluorescence at large positive potentials ($\Delta F/F_{max}$) in double dysgenic/β1 KO myotubes overexpressing the pore mutant α1S (E1014K) and β2a. The data indicate that β2a, upon interaction with the skeletal pore subunit α1S, overrides critical EC coupling determinants present in α1S. We propose that the α1S/β pair, and not the α1S-subunit alone, controls the EC coupling signal in skeletal muscle.

INTRODUCTION

Excitation-contraction (EC) coupling in striated muscle is a fast process in which a brief depolarization causes an immediate elevation of the cytosolic Ca^{2+} (Kim and Vergara, 1998). This process is brought about by a close interaction between the dihydropyridine receptor (DHPR) L-type Ca^{2+} channel and the ryanodine receptor type 1 (RyR1) in skeletal muscle or type 2 (RyR2) in cardiac muscle. Close proximity between the DHPR and RyR complexes occurs at specialized junctions established between the transverse tubular and sarcoplasmic reticulum (SR) membranes (Franzini-Armstrong and Protasi, 1997). At these junctions, voltage-dependent movements of electrical charges in the skeletal DHPR are coupled to the opening of the RyR1 channel. However, the molecular mechanism that opens the RyR1 channel, including which DHPR subunits directly contribute to this process, is, for the most part, unknown. In contrast, activation of RyR2 channels in cardiac muscle is

a Ca^{2+}-dependent process and is strictly proportional to the magnitude of the L-type Ca^{2+} current (Beuckelmann and Wier, 1988; Bers, 2002). This fundamental difference in EC coupling trigger mechanism leads to significant differences in the voltage-dependence of Ca^{2+} transients. In skeletal muscle, the Ca^{2+} transient amplitude versus voltage relationship is sigmoidal whereas in cardiac muscle, it is bell-shaped such that the Ca^{2+} transient is always proportional to the Ca^{2+} current. The biophysical and molecular details of SR Ca^{2+} release mediated by skeletal and cardiac RyR isoforms have been reviewed extensively (McPherson and Campbell, 1993; Coronado et al., 1994; Meissner, 1994; Sutko and Airey, 1996; Fill and Copello, 2002).

In molecular terms, the skeletal DHPR is an $\sim$430-kDa heteropentamer composed of α1S, β1a, α2-δ1, and γ1 subunits. The DHPR α1-subunit belongs to the superfamily of voltage-gated channel proteins with four internal repeats. Electrical charges in the S4 segments in each repeat move outward in response to membrane depolarization. This movement is coupled to the opening of the channel (Bezanilla, 2000). β-subunits are $\sim$65-kDa proteins that bind strongly to the cytosolic loop between repeats I and II of α1 via a conserved $\sim$30-residue β interaction domain or BID (Pragnell et al., 1994; De Waard et al., 1994). β-subunits modulate the kinetics of activation and inactivation of the

Ca^{2+} current (Qin et al., 1996; Wei et al., 2000; Berrou et al., 2001) and strengthen the coupling between S4 charge movements and pore opening (Neely et al., 1993; Olcese et al., 1996; Kamp et al., 1996). The molecular structure and function of the α2-δ1 and γ1 subunits of the skeletal DHPR are far less defined (Gurnett et al., 1996; Ahern et al., 2001c; Arikkath et al., 2003).

Molecular studies of the EC coupling mechanism have relied on myotube models lacking specific DHPR subunits and RyR isoforms. Tanabe et al. (1988) utilized the α1S-null dysgenic myotube to show that the α1S pore subunit was essential for EC coupling signaling. In the dysgenic myotube, a base deletion leads to truncation and degradation of α1S and loss of voltage-activated Ca^{2+} transients. Transfection of cultured dysgenic myotubes with α1S cDNA leads to de novo synthesis of α1S-subunits (Ahern et al., 2001a,d), concentration of the expressed DHPR in EC coupling junctions (Takekura et al., 1994), and recovery of skeletal type EC coupling (Garcia et al., 1994). This expression system permitted studies in which the missing α1S Ca^{2+} pore isoform was replaced by α1C, the cardiac/ brain pore variant (Tanabe et al., 1990). The Ca^{2+} fluorescence versus voltage curve expressed by α1C in dysgenic myotubes had a maximum at $\sim +30$ mV followed by a continuous decrease at more positive potentials. The biphasic nature of this relationship, along with a dependence of Ca^{2+} transients on external Ca^{2+}, showed that Ca^{2+}-dependent EC coupling could be implemented in skeletal myotubes by a hybrid DHPR composed of a cardiac pore subunit and the nonpore subunits expressed endogenously in the dysgenic myotube. The expression of chimeras of α1S and α1C were later used to demonstrate that a domain within the cytosolic loop linking repeats II and III of α1S (α1S L720–Q765) harbored a unique signal essential for skeletal type EC coupling (Nakai et al., 1998a). The studies in dysgenic myotubes have led to the view that the α1S-subunit is the major contributor to the signal transduction and that the α1S II-III loop may be directly responsible for opening RyR1. However, in a strict sense, the observations in dysgenic myotubes cannot exclude the participation of other DHPR subunits in the EC coupling signal since these subunits (α2-δ1, β, γ1) are constitutively expressed in the dysgenic myotube (Arikkath et al., 2003). Hence, if EC coupling domains were to be present in other subunits of the skeletal DHPR, they would have escaped detection in the dysgenic myotube by virtue of being constitutively present. In support of this premise, deletion analysis of the critical α1S L720–Q765 domain suggests that regions other than α1S II-III loop participate in skeletal-type EC coupling (Ahern et al., 2001b).

Gene targeting techniques have substantially increased the number of myotube models that can be used as expression platforms for EC coupling studies. Gregg et al. (1996) described a knockout (KO) of the mouse β1 gene, encoding DHPR β isoforms expressed in skeletal muscle (β1a) and

brain (β1b, β1c) (Powers et al., 1992). The β1 KO mutation, like the dysgenic mutation, is perinatally lethal due to the absence of EC coupling in the skeletal musculature. The β1 KO myotubes fail to contract in response to electrical stimulation despite the presence of normal action potentials, Ca^{2+} storage capacity, and caffeine-sensitive Ca^{2+} release. However, β1 KO cells lack L-type Ca^{2+} current, and depolarization does not produce Ca^{2+} transients (Gregg et al., 1996; Strube et al., 1996). Expression of the skeletal muscle β1a isoform in cultured β1 KO myotubes resulted in the recovery of the wild-type (WT) L-type Ca^{2+} current density, the intramembrane charge movement density, and the amplitude and voltage dependence of Ca^{2+} transients (Beurg et al., 1997). In contrast, expression of the cardiac/brain β2a variant recovered L-type Ca^{2+} currents, but the amplitude of depolarization-activated Ca^{2+} transients was drastically depressed. Because the interaction between the DHPR α1- and β-subunits is essential for cell surface expression (Chien et al., 1995; Bichet et al., 2000), the loss of EC coupling in the β1 KO myotube could be exclusively due to the loss of DHPR voltage sensors from the cell surface. Alternatively, domains of the DHPR β1a-subunit, similar to elements present in the α1S-subunit, might be directly involved in activation of RyR1 channels. To examine the role of DHPR β1a in skeletal-type EC coupling, we chimerized β1a and the cardiac/brain β2a variant and mapped the domain(s) required for functional recovery of skeletal-type EC coupling in cultured β1 KO myotubes (Beurg et al., 1999a,b; Sheridan et al., 2003a). DHPR β-subunits share two conserved central regions amounting to more than half of the total peptide sequence (domains D2 and D4), a nonconserved linker between the two conserved domains (D3), a nonconserved amino terminus (D1), and a nonconserved carboxyl terminus (D5) (Perez-Reyez and Schneider, 1994). We tested the participation of D1, D3, and D5 of β1a in the recovery of Ca^{2+} conductance, charge movements, and EC coupling in β1 KO skeletal myotubes (Beurg et al., 1999a; Sheridan et al., 2003a). Deletion of the D5 region of β1a (β1a residues 470–524) drastically reduced the amplitude of voltage-evoked Ca^{2+} transients without affecting the density of DHPR charge movements. Thus, the membrane density of DHPR voltage sensors, critical for voltage-dependent EC coupling, was not compromised by the carboxyl terminal deletion. On the basis of this result, we have implicated the D5 region of β1a specifically in skeletal-type EC coupling (Sheridan et al., 2003a). Recent recombinant protein binding studies indicate that the D5 domain is essential for strong interaction between DHPR β1a and a specific cytoplasmic region of RyR1 (Cheng and Coronado, 2003).

Targeted disruption of the three mammalian RyR genes has been described (Takeshima et al., 1994, 1996; Nakai et al., 1996; Bertocchini et al., 1997). Two of these variants, namely RyR1 and RyR3, contribute to EC coupling in skeletal muscle. Absence of RyR1 leads to a full loss of skeletal-type EC coupling. Therefore, the RyR1 KO mutation is also

perinatally lethal. Moreover, transient expression of RyR2 or RyR3 in the RyR1-deficient myotube does not lead to a recovery of skeletal EC coupling function (Yamazawa et al., 1996; Nakai et al., 1997; Fessenden et al., 2000). In contrast to RyR1-deficiency, RyR3-deficiency affects dynamic aspects of muscle tension during the embryonic stage and slows Ca^{2+} transient propagation (Bertocchini et al., 1997; Yang et al., 2001). However, RyR3 is not essential for mouse survival. Such a nonequivalent behavior of RyR1 and RyR3 variants suggests that highly specific interactions between RyR1 and the skeletal DHPR are essential for Ca^{2+} signaling in skeletal myotubes. This notion has been corroborated by the identification of RyR1 domains involved in skeletal-type EC coupling using chimeras of RyR1 and RyR2 or RyR1 and RyR3 (Yamazawa et al., 1997; Nakai et al., 1998b; Perez et al., 2003).

In this study, we used KO myotubes lacking DHPR β1, RyR1, and RyR3 to examine the characteristics of the EC coupling induced by the heterologous cardiac/brain β2a variant in the context of myotubes expressing a WT α1S-subunit. This interest was prompted by the observation that many of the carboxyl terminal deletion mutants of the D5 region of β1a, when expressed in β1 KO myotubes, induced Ca^{2+} transients triggered by the Ca^{2+} current (Sheridan et al., 2003a). Hence, the EC coupling mechanism induced by the modified skeletal β1a variants shared many characteristics with the EC coupling process described in the heart. This result begs the question of whether a heterologous DHPR β variant from a gene predominantly expressed in cardiac tissues might be able to transform the skeletal EC coupling process to one more closely resembling cardiac EC coupling. We show that overexpression of the WT cardiac/brain β2a variant (Perez-Reyez and Schneider, 1994) produces drastic changes in EC coupling characteristics of cultured skeletal myotubes, altering it from a purely voltage-dependent process to one controlled mostly by the Ca^{2+} current. The changes are functionally equivalent to those observed in dysgenic myotubes expressing the cardiac/brain α1C variant in the context of the WT DHPR β1a-subunit. The results are consistent with the view that the DHPR β-subunit, like α1, is a key structural determinant of EC coupling in muscle cells. Part of this work has been previously published in abstract form (Sheridan et al., 2002, 2003b).

MATERIALS AND METHODS

Identification of genotypes

We used polymerase chain reaction (PCR) assays to screen for the WT and mutant alleles of the DHPR α1S, β1, RyR1, and RyR3 genes in mice with targeted disruptions of these genes (Gregg et al., 1996; Nakai et al., 1996; Bertocchini et al., 1997) or, in the case of muscular dysgenesis mice (mdg), carrying a frame-shifted α1S-null gene (Chaudhari, 1992). Tail samples were digested with proteinase K (Sigma, St. Louis, MO), and the DNA was then isolated following the Puregene animal tissue protocol (Gentra Systems, Minneapolis, MN). The PCR reactions for each sample were

composed of 11.7 μL distilled water, 1 μL of each 20 μM primer, 3.2 μL of 1.25 mM dNTPs (Stratagene, Cedar Creek, TX), 2 μL 10× PCR buffer (Qiagen, Valencia, CA), 1.2 μL Taq polymerase (Qiagen), and 1 μL of the DNA sample (~100 μg/mL).

DHPR α1S alleles

PCR primers 5′ ttt ccc aca ggc cgt gct gct gct ctt ca 3′ and 5′ gca gct ttc cac tca gga ggg atc cag tgt 3′ were used to amplify a 202-bp fragment of the WT α1S allele. PCR primers 5′ gca gct ttc cac tca gga ggg atc cag tgt 3′ and 5′ ttt ccc aca ggc cgt gct gct gct ctt aga 3′ were used to amplify a 203-bp fragment of the mdg allele (α1S-null). The following conditions apply for the PCR of both DHPR α1S alleles: 1), 2 min at 94°C; 2), 45 s at 94°C; 3), 45 s at 60°C; 4), 1 min at 72°C; 5), cycle through steps 2–4 for 30 times; and 6), 10 min at 72°C.

DHPR β1 alleles

PCR primers 5′ gag aga cat gac aga ctc agc tcg gag a 3′ and 5′ aca ccc cct gcc agt ggt aag agc 3′ were used to amplify a 250-bp fragment of the WT β1 allele. PCR primers 5′ aca ccc cct gcc agt ggt aag agc 3′ and 5′ aca ata gca ggc atg ctg ggg atg 3′ were used to amplify a 197-bp fragment of the KO β1 allele. The following conditions apply for the PCR of both DHPR β1 alleles: 1), 2 min at 94°C; 2), 30 s at 94°C; 3), 45 s at 60°C; 4), 1 min at 72°C; 5), cycle through steps 2–4 for 30 times; and 6), 10 min at 72°C.

RyR1 alleles

PCR primers 5′ gga ctg gca aga gga ccg gag 3′ and 5′ gga agc cag ggc tgc agg tga gc 3′ were used to amplify a 400-bp fragment of the WT RyR1 allele. PCR primers 5′ gga ctg gca aga gga ccg gag 3′ and 5′ cct gaa gaa cga gat cag cag cct ctg ttc c 3′ were used to amplify a 300-bp fragment of the KO RyR1 allele. The following conditions applied for the PCR of both RyR1 alleles: 1), 5 min 30 s at 94°C; 2), 1 min at 94°C; 3), 1 min at 57°C; 4), 1 min at 72°C; 5), cycle through steps 2–4 for 35 times; and 6), 10 min at 72°C.

RyR3 alleles

PCR primers 5′ cac atc cca atc tcc ttt act cc 3′ and 5′ gct tat tct gcc cta atg cca c 3′ were used to amplify a 316-bp fragment of the WT RyR3 allele. PCR primers 5′ ggt cat cct cac ttc gcc tat gtt c 3′ and 5′ cgt gct act tcc att tgt cac gtc 3′ were used to amplify a 920-bp fragment of the KO RyR3 allele. The following conditions apply for the PCR of both RyR3 alleles: 1), 2 min at 94°C (hot start followed by addition of Taq polymerase (Qiagen)); 2), 3 min at 94°C; 3), 1 min at 58°C; 4), 2 min at 72°C; 5), cycle through steps 2–4 for 35 times; and 6), 10 min at 72°C.

Primary cultures

Cultures of myotubes were prepared from hind limbs of E18 fetuses, as described previously (Beurg et al., 1997). Muscles dissected from the fetuses were treated with 0.125% (w/v) trypsin and 0.05% (w/v) pancreatin. After centrifugation, mononucleated cells were resuspended in plating medium containing 78% Dulbeccos's modified Eagle's medium with low glucose (DMEM), 10% horse serum, 10% fetal bovine serum (FBS), and 2% chicken serum extract. Cells were plated on plastic culture dishes coated with gelatin at a density of $\sim 1 \times 10^4$ cells per dish. Cultures were grown at 37°C in 8% CO_2 gas. After myoblast fusion (~6 days), the medium was replaced with FBS free medium, and CO_2 was decreased to 5%.

Double α1S/β1-null myotubes

E18 fetuses lacking α1S and β1a were obtained by screening litters of fetuses from crosses of double heterozygous dysgenic and β1 KO mice

(α1S$^{+/mdg}$, β1$^{+/-}$ × α1S$^{+/mdg}$, β1$^{+/-}$) as described (Ahern et al., 1999; 2003). Mutant fetuses were visually recognized by the absence of muscle movements and were separately processed for myotube cell culture while a PCR screen was conducted in parallel. Limb myotube cultures from double null E18 fetuses with the genotype α1S$^{mdg/mdg}$, β1$^{-/-}$ were utilized in cDNA transfection protocols and are identified in the text as double dysgenic/β1 KO myotubes.

cDNA transfection

cDNA transfection was performed during the myoblast fusion stage with the polyamine LT1 (Panvera, Madison, WI). Cells were exposed for 2–3 h to a transfection solution containing LT1 and cDNA at a 5:1 μg ratio. In addition to the cDNA of interest, cells were cotransfected with a plasmid encoding the T-cell protein CD8, which is used as a transfection marker. Transfected myotubes expressing CD8 were recognized by surface binding of polystyrene beads coated with a monoclonal antibody specific for an external CD8 epitope (Dynal ASA, Oslo, Norway). The efficiency of cotransfection of the marker and the cDNA of interest was ~90%. Whole-cell analysis of Ca^{2+} currents and Ca^{2+} transients was performed 3–5 days after transfection.

cDNA constructs

cDNAs for mouse β1a (residues 1–524; GenBank accession no. NM_031173) and rat β2a (residues 1–604; GenBank accession no. M80545) were subcloned into the pCR-Blunt vector (Invitrogen, Carlsbad, CA), excised by digestion with AgeI and NotI, and cloned into the pSG5 vector in frame with the first 11 residues of the phage T7 gene 10 protein for antibody tagging. The α1S (E1014K) substitution was introduced in a rabbit α1S template (GenBank accession no. M23919) and was described previously (Ahern et al., 2001b). WT α1S and α1S (E1014K) were fused in-frame to the first 11 amino acids of the phage T7 gene 10 protein in the pSG5 vector.

Whole-cell voltage clamp

Whole-cell recordings were performed as described previously (Strube et al., 1996) with an Axopatch 200B amplifier (Axon Instruments, Foster City, CA). Effective series resistance was compensated up to the point of amplifier oscillation with the Axopatch circuit. All experiments were performed at room temperature. The external solution was (in mM) 130 TEA methanesulfonate, 10 CaCl$_2$, 1 MgCl$_2$, 10^{-3} TTX, 10 HEPES titrated with TEA(OH) to pH 7.4. The pipette solution consisted of (in mM) 140 Cs aspartate, 5 MgCl$_2$, 0.1 EGTA (when Ca^{2+} transients were recorded) or 5 EGTA (when only Ca^{2+} currents were recorded), and 10 MOPS titrated with CsOH to pH 7.2. Patch pipettes had a resistance of 1–1.5 MΩ when filled with the pipette solution. The limit of Ca^{2+} current detection was ~20 pA/cell or ~0.05 pA/pF for the smallest cells having the lowest capacitive noise.

Confocal fluorescence microscopy

Confocal line scan measurements were performed as described previously (Conklin et al., 1999). All experiments were performed at room temperature. Cells were loaded with 5 μM fluo-4 acetoxymethyl (AM) ester (Molecular Probes, Eugene, OR) for 60 min at room temperature. Cells were viewed with an inverted Olympus microscope with a 20× objective (N.A. = 0.4) and a Fluoview confocal attachment (Olympus, Melville, NY). A 488-nm spectrum line for fluo-4 excitation was provided by a 5-mW Argon laser attenuated to 6% with neutral density filters. For voltage-activated Ca^{2+} transients, line scans consisted of 1000 lines, each of 512 pixels, acquired at a rate of 2.05 milliseconds per line. Line scans were synchronized to start 100 ms before the onset of the depolarization. For Ca^{2+} transients activated by caffeine or CMC (4-chloro-m-cresol, Sigma, St. Louis, MO), line scans

consisted of 1000 lines, each of 512 pixels, acquired at a rate of 30.8 milliseconds per line. Line scans were synchronized to start 800 ms before the onset of the external solution change. The time course of the space-averaged fluorescence intensity change and $\Delta F/F$ units were estimated as follows: 1), The pixel intensity in a line scan was transformed into arbitrary units, and the mean intensity of each line was obtained by averaging pixels covering the cell exclusively; 2), The mean resting fluorescence intensity (F) corresponds to the mean intensity of each line averaged before stimulation and was used as a baseline; 3), The change in mean line intensity above baseline (ΔF) was obtained by subtraction of F (baseline) from the mean line intensity; 4), ΔF was divided by the baseline F for each line in a line scan and was plotted as a function of time. The peak-to-peak noise in the baseline fluorescence averaged ~0.1 $\Delta F/F$ units which was previously estimated to correspond approximately to a 200-nM change in free Ca^{2+} (Conklin et al., 1999). Since $\Delta F/F$ was spatially averaged, noise varied with spatial inhomogeneities in fluo-4 fluorescence and cell size. The smallest fluorescence signals reported in this study were ~0.2 $\Delta F/F$ in β2a-overexpressing RyR1/RyR3 KO myotubes and ~0.4 $\Delta F/F$ in β2a-overexpressing RyR1 KO myotubes (Table 2). To construct peak Ca^{2+} fluorescence versus voltage curves, we used the highest $\Delta F/F$ line value after the onset of the pulse and up to the termination of the pulse. Image analyses were performed with NIH Image software (National Institutes of Health, Bethesda, MD). To obtain reliable Ca^{2+} transient versus voltage curves, seven-step depolarizations of 50 ms or 200 ms were applied in descending order (from +90 mV to −30 mV) from a holding potential of −40 mV. Between each depolarization, the cell was maintained at the resting potential for 30 s to permit recovery of the resting fluorescence.

Immunostaining

Four to five days after transfection, cells were fixed in 100% methanol and processed for immunostaining as described previously (Gregg et al., 1996). The primary antibody was a mouse monoclonal against the T7 epitope (Novagen, Madison, WI) present in β1a and β2a and was used at a dilution of 1:1000. The secondary antibody was a fluorescein conjugated polyclonal goat anti-mouse IgG (Boehringer Mannheim, Indianapolis, IN) and was used at a dilution of 1:1000. Confocal images of 0.3 to 0.4 microns per pixel were obtained in the Olympus Fluoview using a 40× oil-immersion objective (N.A. = 1.3). Images were Kalman-averaged 3 times, and the pixel intensity was displayed as 16 levels of gray in reverse. All images were acquired with minimal laser power (6% of maximum 5 mW) and predetermined PMT settings to avoid pixel saturation and for accuracy in the comparison of images.

Curvefitting

The voltage dependence of the Ca^{2+} conductance and peak fluorescence, assayed with the 50-ms depolarization, was fitted in all cases according to a Boltzmann distribution (Eq. 1)

$$A = A_{max}/(1 + \exp(-(V - V1/2)/k))$$

where A_{max} is G_{max} or $\Delta F/F_{max}$, $V1/2$ is the potential at which $A = A_{max}/2$, and k is the slope factor. For myotubes overexpressing β1a, the voltage dependence of peak fluorescence assayed with a 200-ms depolarization was fit with Eq. 1. The β2a variant produced biphasic bell-shaped fluorescence versus voltage curves with varying degrees of curvature. For myotubes overexpressing β2a, the voltage dependence of peak intracellular Ca^{2+} assayed with a 200-ms depolarization was fit with the modified Boltzmann distribution (Eq. 2)

$$\Delta F/F = (V - Vr)/k'[\Delta F/F_{max}/(1 + \exp(V - V1/2)/k)],$$

where $(V - Vr)$ is a factor that accounts for the decrease in Ca^{2+} current trigger at positive potentials and k' is a scaling factor that varies with the magnitude of $\Delta F/F_{max}$. Other parameters are the same as in Eq. 1.

Parameters of a fit of averages of many cells (population average) are shown in figures. The statistics of parameters of the fit of individual cells are shown in Table 1. Student's t-tests and analysis of variance (ANOVA) were performed with Analyze-it software (Analyze-it, Leeds, UK).

RESULTS

Previous studies showed that β1 KO myotubes expressing the heterologous DHPR β2a-subunit had weak Ca^{2+} transients compared to controls expressing the skeletal muscle-specific β1a-subunit (Beurg et al., 1999a,b; Sheridan et al., 2002, 2003b). Here we demonstrate that β2a induces Ca^{2+} transients triggered by the Ca^{2+} current, and furthermore, both RyR isoforms described in primary skeletal myotubes are implicated in the functional changes. To separate the contributions of RyR1 and RyR3, we characterized functional expression of β2a in cultured primary myotubes from RyR1 KO, RyR3 KO, and double RyR1/RyR3 KO mice. Interbreeding mice heterozygous of the RyR1 KO allele and homozygous for the RyR3 KO allele produced RyR1/RyR3 KO mice (Ikemoto et al., 1997; Barone et al., 1998; Conklin et al., 2000). Genotypes were screened by PCR as described in Materials and Methods. Additional controls were performed in β1 KO myotubes lacking the endogenous β1a variant. The two DHPR β variants investigated, namely the heterologous rat β2a and the homologous mouse β1a used as a reference, carried a T7 epitope tag fused to the amino terminus for determining relative levels of protein expression in transfected cells. Fig. 1 shows confocal anti-T7 immunofluorescence in four myotube genotypes expressing the homologous and heterologous DHPR β variants. The cDNA of interest was cotransfected with the CD8 cDNA, which was used to identify viable transfected myotubes in voltage-clamp experiments. Dishes of transfected cells were incubated with anti-CD8 antibody beads, fixed, and processed for immu-

nostaining with anti-T7 antibody. Protein expression was determined 4–5 days after transfection. Voltage-clamp experiments have determined that this transfection time is adequate for full functional recovery of EC coupling properties in β1 KO myotubes (Beurg et al., 1997). At this stage of protein expression, we found abundant β-protein throughout the myotube with the exclusion of the cell nuclei. Based on fluorescence intensity, we estimated that all myotube genotypes overexpressed exogenous β2a and β1a proteins at comparable levels.

Transcripts for RyR3 have been detected in primary cell cultures of WT and RyR1 KO limb myotubes (Takeshima et al., 1995). Furthermore, functional RyR3 channels account for caffeine-induced Ca^{2+} release and Ca^{2+} sparks detected in embryonic RyR1 KO myotubes (Takeshima et al., 1995; Conklin et al., 2000). In contrast, RyR3 has been reported to be absent in a myogenic cell line derived from RyR1 KO embryonic limb myotubes (Fessenden et al., 2000). To determine whether one or two RyR variants were present in our primary cell cultures, we conducted Ca^{2+} release studies using caffeine and the high-affinity RyR1 agonist CMC (Herrmann-Frank et al., 1996). In these experiments, cells were loaded with fluo-4 AM, and SR Ca^{2+} release was induced by fast perfusion of external solution supplemented with caffeine (10 mM) or CMC (0.5 mM). The perfusion solution was passed through a large-bore pipette placed near the cell with the pipette connected to a pressurized manifold (ALA Scientific, Westbury, NY) and synchronized to confocal line scan image acquisition. Fig. 2 shows Ca^{2+} transients evoked by fast perfusion of caffeine or CMC in WT, RyR3 KO, RyR1 KO, and RyR1/RyR3 KO myotubes. As indicated by the line diagram above each trace of fluorescence, the external solution change lasted 4 s and was initiated 800 ms after the start of the line scan. After the pulse of agonist, line scan acquisition was continued for an additional 26 s. The time course of the space-averaged confocal fluorescence intensity was computed from the line scan image and is shown in $\Delta F/F$ units. A rapid increase in myotube fluorescence was observed in response to caffeine in WT and RyR3 KO myotubes. Comparatively weaker and slower responses to caffeine were present in ~60% of the tested RyR1 KO myotubes (26 of 41 cells) with the rest entirely unresponsive to caffeine. Caffeine had no effect in double RyR1/RyR3 KO myotubes (14 of 14 cells). The presence of caffeine-sensitive Ca^{2+} pools in RyR1 KO and RyR3 KO, but not in RyR1/RyR3 KO myotubes, confirmed the presence of these two RyR isoforms in our cell cultures and was consistent with previous studies (Takeshima et al., 1995; Conklin et al., 2000). However, since the response to caffeine in RyR1 KO myotubes was heterogeneous, functional RyR3 channels may not be present in all RyR1-deficient cells. Alternatively, RyR3 channels may not be responsive to caffeine in all cells for some unknown reason. Fig. 2 also shows that large and fast responses to CMC were observed in WT and RyR3 KO myotubes, and much weaker

TABLE 1 Parameters of the Ca^{2+} conductance expressed by DHPR β1a and β2a in skeletal myotubes

	G_{max} (pS/pF)	$V1/2$ (mV)	k (mV)
WT	186 ± 13 (28)	12 ± 2	5.6 ± 0.3
β1 KO + β1a	195 ± 23 (10)	15 ± 2	4.5 ± 0.6
RyR3 KO + β1a	162 ± 15 (9)	17 ± 2	4.4 ± 0.6
RyR1 KO + β1a	26 ± 6* (4)	18 ± 3	7.2 ± 1.1
RyR1/RyR3 KO + β1a	36 ± 10* (3)	27 ± 1	5.7 ± 1.1
β1 KO + β2a	184 ± 36 (6)	11 ± 1	5.1 ± 0.3
RyR3 KO + β2a	156 ± 21 (6)	11 ± 2	3.8 ± 0.4
RyR1 KO + β2a	189 ± 19 (13)	12 ± 2	5.1 ± 0.2
RyR1/RyR3 KO + β2a	158 ± 23 (10)	13 ± 4	5.6 ± 0.3

Entries correspond to the mean ± SE of Boltzmann parameters (G_{max}, $V1/2$, and k) fitted to each cell, according to Eq. 1. The number of cells is in parentheses. For statistical analysis, parameters of WT, all β1a-transfected and all β2a-transfected genotypes were compared to β1a-transfected β1 KO myotubes. Asterisks indicate data in each column with 1-way ANOVA significance $p < 0.05$.
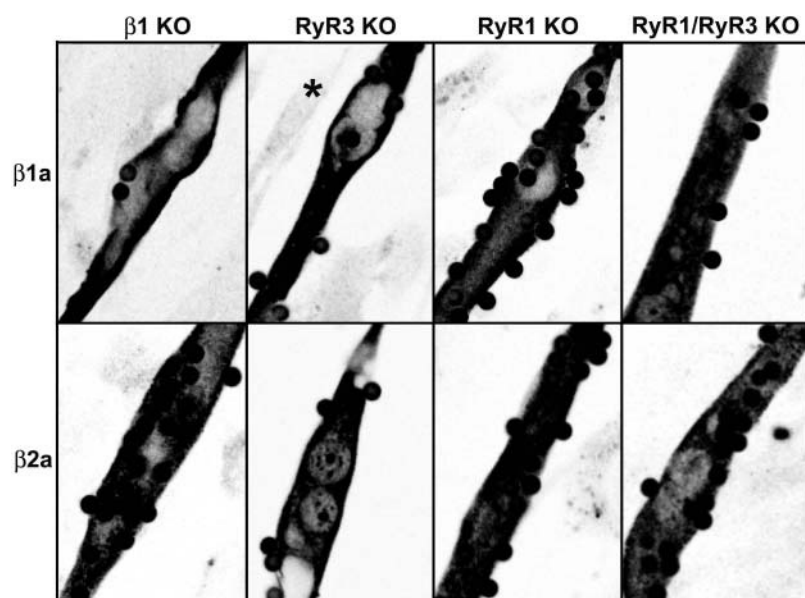
FIGURE 1 β-protein expression in β1 KO and RyR KO myotubes. Confocal immunofluorescence of myotubes expressing T7-tagged DHPR β1a- or β2a-subunits. Cells with the indicated genotype were transfected with CD8 cDNA plus the β1a or β2a cDNA. β1a corresponds to the full-length mouse cDNA; β2a corresponds to the full-length rat cDNA. Cells were incubated with CD8 antibody beads, fixed, and stained with anti-T7 primary/fluorescein-conjugated secondary antibodies. Pixel intensity was converted to a 16-level inverted gray scale with high-intensity pixels in black color. Images are 84 × 56 microns and on-focus beads are 4.5 microns in diameter. The asterisk indicates a nontransfected myotube in the same focal plane as the transfected cell.

and slower responses were present in RyR1 KO and double RyR1/RyR3 KO myotubes. The results in RyR3 KO compared to RyR1 KO myotubes agreed with previous determinations showing that CMC is predominantly a RyR1 agonist (Fessenden et al., 2000). Yet, the presence of a small but consistent response to CMC in double RyR1 KO/ RyR3 KO myotubes (15 of 15 cells) implicates targets other than RyRs, at least in myotubes in which both RyR isoforms are absent. Histograms of the mean maximal fluorescence induced by caffeine and CMC and the time to maximal fluorescence after agonist exposure are shown at the bottom of Fig. 2. Asterisks indicate ANOVA significance $p < 0.05$ relative to WT. The absence of a response to caffeine in double KO myotubes provided a null background against which the responses in RyR1 KO and RyR3 KO myotubes could be compared. We observed a higher peak and faster time-to-peak responses to caffeine in RyR3 KO than in RyR1 KO myotubes, relative to the null background. This suggested that RyR3 KO cells had a higher sensitivity to caffeine than RyR1 KO cells. Alternatively, RyR3 KO cells expressed a higher density of RyR1 receptors than the density of RyR3 receptors expressed in RyR1 KO cells. Since 10 mM caffeine was reported to saturate responses in myotubes expressing either RyR1 or RyR3 (Fessenden et al., 2000), it is likely that the differential sensitivity to caffeine reflects differences in the functional density of RyRs with RyR1 present at a much higher density than RyR3, respectively, in RyR3 KO and RyR1 KO myotubes. It is also possible that RyR1 expression may be up-regulated in RyR3 KO myotubes relative to WT since CMC responses were significantly higher in the former than the latter. In summary, the Ca^{2+} release responses to caffeine and CMC show that functional RyR1 and RyR3 are present, respectively, in RyR3 KO and most RyR1 KO cultured myotubes.

Fig. 3 shows Ca^{2+} conductance versus voltage relationships in myotubes transfected with each of the two DHPR β isoforms (β1a and β2a in top and bottom rows, respectively) in each of four genotypes (β1 KO, RyR3 KO, RyR1 KO, and RyR1/RyR3 KO in columns from left to right). β2a-transfected myotubes were compared to β1a-transfected myotubes even though both RyR KO genotypes are likely to express a native DHPR that includes β1a. We felt that in the case of the RyR KO genotypes, myotubes with exogenous β1a overexpression provided a better control than nontransfected myotubes since overexpression eliminated potential phenotypic changes introduced by an unknown up- or down-regulation of endogenous β1a. However, this concern was largely unfounded. The insets show whole-cell Ca^{2+} currents elicited by 500-ms depolarizations to -10 and $+30$ mV from a holding potential of -40 mV. The complete pulse protocol utilized for fitting conductance versus voltage curves consisted of 500-ms step depolarizations from -35 mV to $+60$ mV every 5 mV. The gray lines in each plot indicate the mean conductance of nontransfected myotubes. We found that nontransfected β1 KO myotubes had marginally detectable Ca^{2+} currents in agreement with previous studies (Ahern et al., 2003). In β1a-expressing β1 KO myotubes, we consistently detected a high-density Ca^{2+} current with a maximal conductance, G_{max}, and other Boltzmann parameters, similar to those of WT myotubes (Table 1). Thus, as shown previously (Beurg et al., 1997), β1a overexpression in the β1 KO myotube recovered the normal Ca^{2+} current phenotype. Furthermore, the Ca^{2+} current density of WT myotubes was similar to that reported previously by others and us (Beurg et al., 1997; Strube et al., 1998; Avila and Dirksen, 2000). Averages of Boltzmann parameters fitted to the conductance versus voltage curve of each cell and the statistical significance of the data are shown
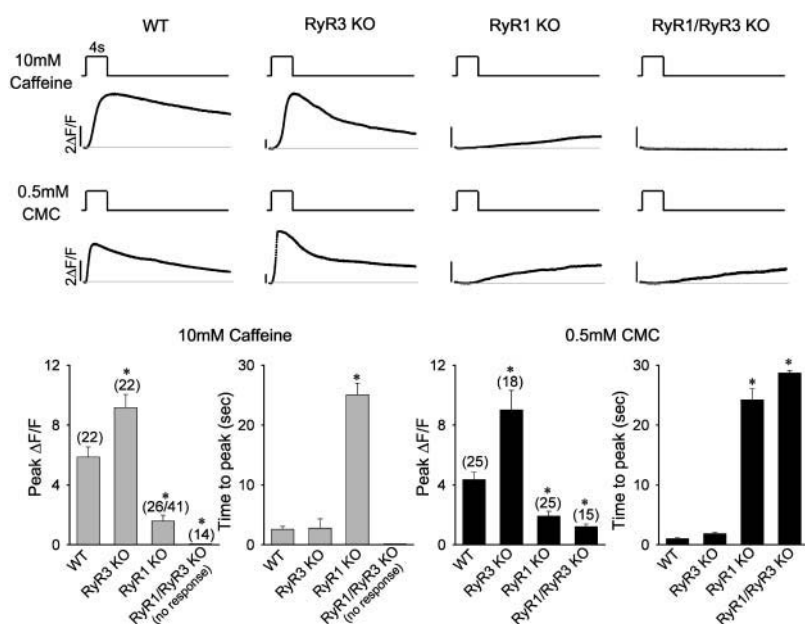
FIGURE 2 SR Ca^{2+} release induced by caffeine and CMC in WT and RyR KO myotubes. Time course of confocal fluo-4 fluorescence is shown for nontransfected myotubes of the indicated genotype: normal (WT), RyR3 KO, RyR1 KO, and double RyR1/RyR3 KO. Different cells were used to elicit responses to caffeine (*top row*) and CMC (*bottom row*). The line diagrams indicate rapid perfusion for 4 s of external solution with 10 mM caffeine or 0.5 mM CMC with a total line scan duration (*x* axis) of 30.8 s. Traces show the time course of the spatial integral of the line scan image fluorescence in $\Delta F/F$ units. Note differences in $\Delta F/F$ scales. Histograms show Ca^{2+} release responses to caffeine (*left*) and CMC (*right*). The maximal confocal fluorescence in $\Delta F/F$ units (mean $\pm$ SE) is shown after myotube exposure to 10 mM caffeine (*left*) or 0.5 mM CMC (*right*). The time to maximal fluorescence (mean $\pm$ SE) is shown within a 30.8-s line scan after agonist perfusion. The numbers in parentheses indicate the number of tested cells. None of the tested RyR1/RyR3 KO myotubes ($n = 14$) responded to caffeine; 26 of 41 RyR1 KO myotubes tested responded to caffeine, and statistics are provided for caffeine-sensitive cells; all WT and RyR3 KO myotubes tested responded to caffeine and CMC; and all RyR1 KO and RyR1/RyR3 KO myotubes tested responded to CMC. Asterisks indicate statistical significance $p < 0.01$ in one-way ANOVA against WT.

in Table 1. Overexpression of β1a in the RyR3 KO myotube did not increase Ca^{2+} current density beyond that present in nontransfected RyR3 KO myotubes, which was entirely normal ($G_{max} = 182 \pm 15$ pS/pF, $n = 4$ cells versus 162 ± 15 pS/pF, $n = 9$ cells for nontransfected and β1a-transfected, respectively). In RyR1 KO and RyR1/RyR3 KO myotubes, the endogenous Ca^{2+} current density was severely depressed, and β1a overexpression failed to increase it beyond levels present in nontransfected cells. The G_{max} of nontransfected RyR1 KO and RyR1/RyR3 KO myotubes were 27 ± 5 pS/pF (14 cells) and 24 ± 10 pS/pF (4 cells), respectively. These values were statistically similar to the density of β1a-transfected RyR1 KO and RyR1 KO/RyR3 KO myotubes shown in Table 1. The inability of exogenous β1a overexpression to increase the Ca^{2+} current density in RyR1-deficient myotubes was not surprising in light of the known fact that RyR1 is a strong enhancer of the native DHPR Ca^{2+} current (Nakai et al., 1996; Avila et al., 2001; Ahern et al., 2003). Thus, absence of RyR1, and not the endogenous level of the DHPR β1a-subunit, may be the limiting factor for Ca^{2+} current expression in the RyR1-deficient genotypes. In β1 KO myotubes, β2a expressed a high-density Ca^{2+} current with a G_{max} similar to that recovered by β1a (Table 1). Moreover, the half-activation potential and voltage dependence of the Ca^{2+} current expressed by the β1a and β2a were also similar. Also, previous studies had shown that Ca^{2+} currents recovered by β1a and β2a had similar mean-variance noise characteristics and activation kinetics (Beurg et al., 1999b). Hence it is highly likely that β2a became integrated into a functional skeletal DHPR with the pore subunit α1S providing the

pathway for the Ca^{2+} current. The fate of the two other subunits of the DHPR in this hybrid complex is not known. However, their presence in the complex is suggested by the complete normalcy of the Boltzmann parameters of the Ca^{2+} conductance recovered by β2a (Table 1). β2a overexpression in RyR1 KO myotubes was recently shown to restore a slow Ca^{2+} current with an entirely WT density (Ahern et al., 2003). The bottom row of Fig. 3 confirmed this observation and further showed that β2a recovered high-density Ca^{2+} currents in all genotypes analyzed, including double RyR1/RyR3 KO myotubes. In the RyR1 KO and RyR1 KO/RyR3 KO myotubes, β2a recovered Ca^{2+} currents with a density $\sim$5 fold larger than that present in nontransfected cells and similar to that of WT myotubes (Table 1). Thus, in contrast to the behavior of β1a, Ca^{2+} currents recovered by β2a readily bypassed the inhibition imposed by the absence of RyR1. Furthermore, the results in double KO myotubes showed that neither RyR1 nor RyR3 were required for DHPR Ca^{2+} current expression when the heterologous β2a-subunit was present in the DHPR complex. Given this drastic change in Ca^{2+} current expression pattern, we further tested if β2a was capable of recruiting a pore subunit other than α1S which could potentially be present in the cultured myotube and that could account for the Ca^{2+} currents recovered by β2a. Controls indicated that neither β1a nor β2a recovered Ca^{2+} currents when overexpressed in α1S-null dysgenic myotubes in similar cell culture conditions (not shown). Thus, non-α1S pore subunits, if present in skeletal myotubes, may not be able to combine with β1a or β2a to generate functional Ca^{2+} channels. This result strongly suggested that Ca^{2+} currents
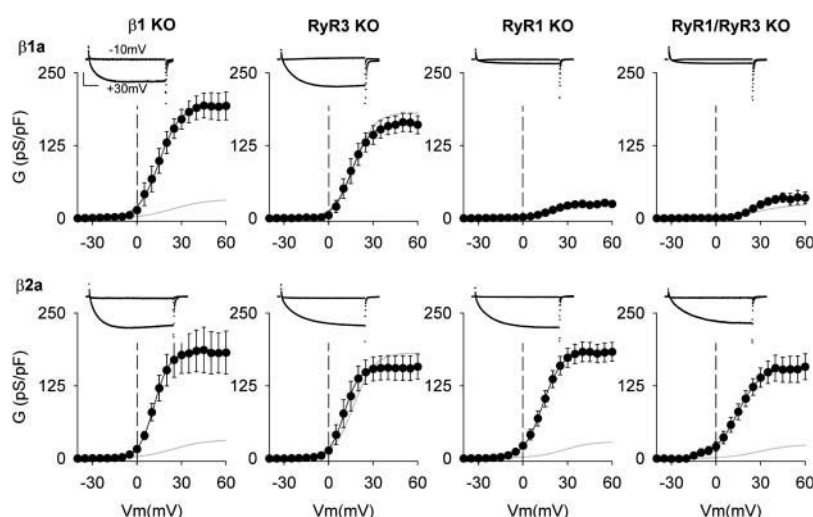
FIGURE 3 Ca^{2+} conductance expressed by the heterologous DHPR β2a-subunit in β1 KO and RyR KO myotubes. Myotubes with the indicated genotype (β1 KO, RyR3 KO, RyR1 KO, and double RyR1/RyR3 KO) were transfected with β1a (*top row*) or β2a (*bottom row*). Insets show representative Ca^{2+} currents at -10 mV and $+30$ mV for a depolarization of 500 ms from a holding potential of -40 mV. Lines correspond to a Boltzmann fit of the population mean Ca^{2+} conductance indicated in Table 1. All conductance versus voltage curves were fit with Eq. 1. Parameters of the fitted lines, with G_{max} in pS/pF, V1/2 in mV, and k in mV, were as follows: for β1 KO myotubes, were 194, 14.9, and 7 for β1a overexpression and 183, 11.6, and 5.2 for β2a overexpression; for RyR3 KO myotubes, were 162, 15.5, 6.1 for β1a and 156, 10.5, 5 for β2a; for RyR1 KO myotubes were 25, 17.9, 6.6 for β1a and 184, 13.2, 6.4 for β2a; for RyR1/RyR3 KO myotubes were 35, 25.8, 5.8 for β1a and 157, 14.6, 8 for β2a.

recovered by β2a in RyR1 KO and RyR1/RyR3 KO myotubes originated from hybrid DHPR complexes that included α1S and the exogenous β2a-subunit. A mechanism explaining how Ca^{2+} currents recovered by β2a bypass the requirement for RyR1 has been proposed elsewhere (Ahern et al., 2003).

In β1 KO myotubes overexpressing β1a, the Ca^{2+} current has no bearing on the magnitude of the Ca^{2+} transient (Beurg et al., 1997). However, recent studies showed that long depolarizations significantly increased the total Ca^{2+} entering the cell, and that the excess of Ca^{2+} entry triggered SR Ca^{2+} release when β1 KO myotubes overexpressed truncated variants of β1a (Sheridan et al., 2003a). For this reason, possible changes in EC coupling produced by β2a overexpression were tested by voltage steps with a duration of 50 ms and 200 ms in the range of -30 mV to $+90$ mV, which covered both the inward and outward phases of the myotube Ca^{2+} current. Fig. 4 shows confocal Ca^{2+} transients in response to 200-ms depolarizations to $+30$ and $+90$ mV from a holding potential of -40 mV in the same myotube. Ca^{2+} currents were acquired concurrently, and they were similar in density to those described in Fig. 3. The entire pulse protocol consisted of 50-ms and 200-ms depolarizations, and a comparison of Ca^{2+} transients stimulated by the two protocols is described below. Because the Ca^{2+} current becomes progressively smaller at potentials >30 mV, as the imposed voltage approaches the Ca^{2+} current reversal potential and the Ca^{2+} equilibrium potential, a contribution of the Ca^{2+} current as trigger of the Ca^{2+} transient can be readily deduced by comparing Ca^{2+} transients at $+30$ mV and $+90$ mV. Fig. 4 shows that in β1 KO cells overexpressing β1a, Ca^{2+} transients had a nearly identical shape and magnitude at $+30$ and $+90$ mV. This result was consistent with the previous data (Beurg et al., 1999a,b; Sheridan et al., 2003a) and the well-known voltage dependence of skeletal-type EC coupling, which is

unrelated to the fate of the Ca^{2+} current (Rios and Pizarro, 1991). Similarly, Ca^{2+} transients in β1a-expressing RyR3 KO myotubes had the same maximal intensity at $+30$ and $+90$ mV, and this result agreed with previous determinations showing that RyR3 KO myotubes display skeletal-type EC coupling (Dietze et al., 1998). In myotubes lacking RyR1 (RyR1 KO and RyR1/RyR3 KO), β1a overexpression failed to recover Ca^{2+} transients, which is not surprising since RyR3 is incapable of supporting skeletal-type EC coupling (Fessenden et al., 2000). Additionally, the Ca^{2+} current density in the RyR1-deficient genotypes is noticeably small. Hence, Ca^{2+}-dependent Ca^{2+} release or a direct contribution of the Ca^{2+} current to the cell fluorescence would be difficult to detect in these cells. In contrast, Ca^{2+} transients of various magnitudes were detected in all myotube genotypes overexpressing β2a and were two- to fivefold smaller at $+90$ than at $+30$ mV (Fig. 4, *bottom row*). Furthermore, in RyR1 KO and RyR1/RyR3 KO myotubes, β2a-mediated Ca^{2+} transients were seen at $+30$ but not at $+90$ mV, suggesting that a significant proportion of the fluorescence signal in these myotubes could arise from the Ca^{2+} current itself. β2a-mediated Ca^{2+} transients in β1 KO myotubes were smaller in magnitude than those in β1a-expressing β1 KO, in agreement with previous determinations (Beurg et al., 1999b). In addition, the selected β2a-expressing RyR3 KO myotube shows Ca^{2+} transients larger than that of the β2a-expressing β1 KO myotube. However, on average, this difference was not significant (Table 2). The results in β1 KO and RyR3 KO myotubes suggested that β2a expression changed the EC coupling signal from one that is controlled by voltage to one in which the Ca^{2+} current served as a trigger. We were especially surprised by the changes in the voltage dependence of Ca^{2+} transients in RyR3 KO myotubes since nontransfected RyR3 KO myotubes (Dietze et al., 1998) or β1a-overexpressing RyR3 KO myotubes (Fig. 4, *top row*) showed bona fide skeletal-type EC
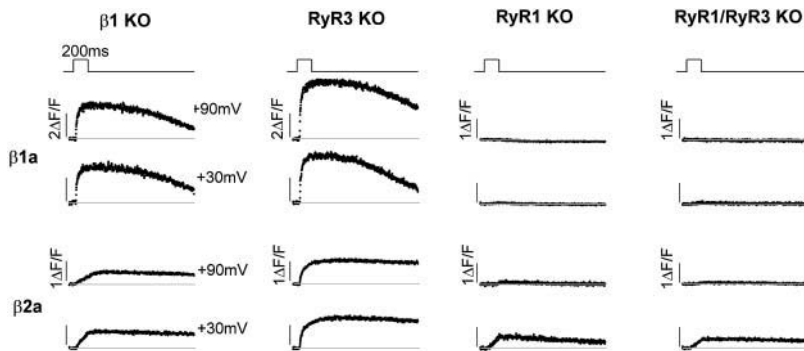
FIGURE 4 Ca^{2+} transients expressed by the heterologous DHPR β2a-subunit in β1 KO and RyR KO myotubes. Myotubes with the indicated genotype (β1 KO, RyR3 KO, RyR1 KO, and double RyR1/RyR3 KO) were transfected with β1a (*top row*) or β2a (*bottom row*). Ca^{2+} transients were elicited by step depolarizations to +30 and +90 mV. Myotubes were held at a resting potential of −40 mV and depolarized for 200 ms. The time course of the cell fluorescence was obtained by integration of the line scan image as described in Materials and Methods. Note differences in ΔF/F scales.

coupling. This result seemed to indicate that β2a behaved as a negative dominant subunit capable of disrupting normal DHPR function in the RyR3 KO myotube.

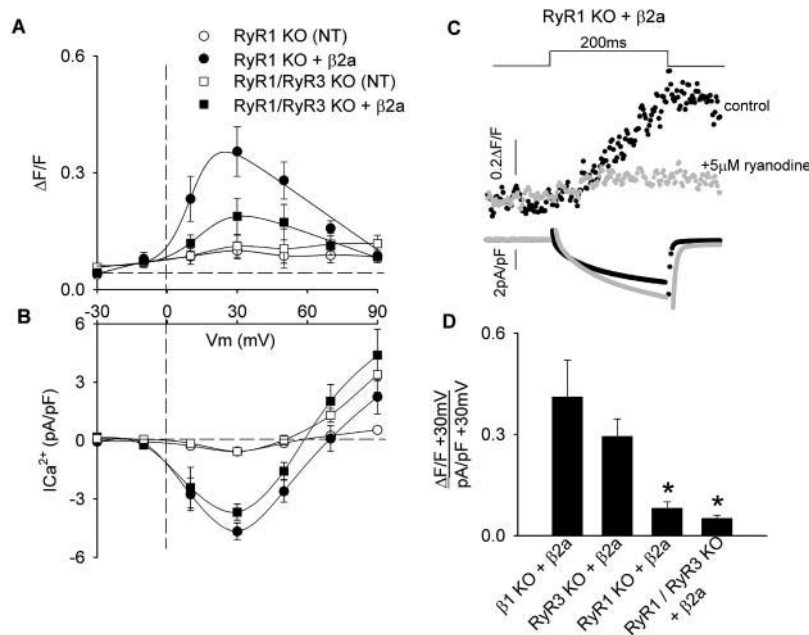To determine how much of the fluorescence signal in β2a-expressing myotubes was due to the Ca^{2+} current and how much was due to SR Ca^{2+} release, we examined fluorescence versus voltage and Ca^{2+} current versus voltage relationships acquired concurrently. Fluorescence signals in RyR1/RyR3 KO myotubes should exclusively reflect the contribution of the Ca^{2+} current, whereas those in RyR1 KO should reflect the contribution of the Ca^{2+} current and Ca^{2+} entry dependent Ca^{2+} release mediated by RyR3. Consistent with this idea, Fig. 5 A shows that β2a-mediated Ca^{2+} transients in RyR1 KO (*closed circles*) and RyR1 KO/RyR3 KO (*closed squares*) myotubes had a bell-shaped dependence with a maximum at +30 mV, which coincided with the maximal Ca^{2+} current shown in Fig. 5 B. Additionally, the peak ΔF/F at +30 mV was larger in RyR1 KO than in RyR1 KO/RyR3 KO myotubes, whereas the Ca^{2+} current density was similar in both cases. The baseline for these curves was provided by the behavior of nontransfected RyR1 KO myotubes (*open circles*) and RyR1/RyR3 KO myotubes

(*open squares*), which lacked Ca^{2+} transients entirely and expressed a minimal Ca^{2+} current. The peak ΔF/F of nontransfected myotubes was undistinguishable from the noise of the measurement, which was ~0.1 ΔF/F (see Materials and Methods). We surmise that the excess in cell fluorescence in β2a-expressing RyR1 KO myotubes, above that present in β2a-expressing RyR1 KO/RyR3 KO myotubes, should reflect SR Ca^{2+} release due to Ca^{2+}-dependent activation of RyR3. To confirm this idea, β2a-expressing RyR1 KO myotubes were treated with 5 μM ryanodine to block any RyR-dependent SR Ca^{2+} release. Fig. 5 C shows representative Ca^{2+} transients and Ca^{2+} currents at +30 mV in a β2a-expressing RyR1 KO myotube (*black traces*) and in a separate β2a-expressing RyR1 KO myotube treated with ryanodine (*gray traces*). To ensure a complete elimination of the fluorescence change due to EC coupling, myotubes were exposed to ryanodine for 30 min. For this reason, controls and ryanodine-treated cells were different. Myotubes were selected so that the Ca^{2+} current densities were approximately the same. Ryanodine treatment significantly reduced the fluorescence signal in β2a-expressing RyR1 KO myotubes and suggested that a significant

TABLE 2 Parameters of Ca^{2+} transients expressed by DHPR β1a and β2a in skeletal myotubes

	50 ms				200 ms			
	$ΔF/F_{max}$	V1/2(mV)	k(mV)	$\frac{ΔF/F(exp\ max)}{ΔF/F + 90\ mV}$	$ΔF/F_{max}$	V1/2(mV)	k(mV)	$\frac{ΔF/F(exp\ max)}{ΔF/F + 90\ mV}$
WT	2.6 ± 0.4 (12)	4 ± 3	8.4 ± 1.0	1.1 ± 0.1	2.8 ± 0.4 (9)	8 ± 3	9.3 ± 2.1	1.1 ± 0.1
β1 KO + β1a	2.7 ± 0.5 (10)	−3 ± 2	7.7 ± 0.5	1.0 ± 0.1	3.4 ± 0.6 (10)	−8 ± 2	5.8 ± 1.1	1.2 ± 0.1
RyR3 KO + β1a	2.2 ± 0.4 (10)	−6 ± 2	8.6 ± 1.1	1.2 ± 0.1	3.3 ± 0.6 (9)	−9 ± 2	7.2 ± 1.4	1.2 ± 0.1
RyR1 KO + β1a	− (5)	−	−	−	− (7)	−	−	−
RyR1/RyR3KO + β1a	− (4)	−	−	−	− (5)	−	−	−
β1 KO + β2a	0.9 ± 0.2* (10)	−2 ± 3	7.4 ± 1.5	1.5 ± 0.1*	1.7 ± 0.4* (10)	6 ± 3	7.6 ± 1.9	2.3 ± 0.4*
RyR3 KO + β2a	0.6 ± 0.1* (8)	8 ± 4	9.4 ± 1.3	1.2 ± 0.1	1.9 ± 0.3* (14)	4 ± 3	7.1 ± 0.9	1.3 ± 0.1
RyR1 KO + β2a	− (5)	−	−	−	0.4 ± 0.1* (5)	6 ± 2	6.3 ± 1.0	4.5 ± 0.9*
RyR1/RyR3KO + β2a	− (3)	−	−	−	0.2 ± 0.1* (7)	12 ± 4	9.2 ± 0.4	2.6 ± 0.4*

Mean ± SE of Boltzmann parameters fitted to each cell with number of cells in parentheses. $ΔF/F_{max}$, V1/2, and k are parameters of the Boltzmann fit. Parameters of fluorescence versus voltage curves are shown for 50-ms and 200-ms depolarizations. All data from β1a-expressing myotubes and 50-ms data from myotubes expressing β2a were fit with Eq. 1. The 200-ms data from myotubes expressing β2a was fit with Eq. 2. ΔF/F (*exp max*) corresponds to the experimental maximal ΔF/F for a given fluorescence versus voltage curve. ΔF/F +90 mV corresponds to the experimental ΔF/F at +90 mV. For statistical analysis, parameters of WT, all β1a-transfected, and all β2a-transfected genotypes were compared to β1a-transfected β1 KO myotubes. Asterisks indicate data in each column with 1-way ANOVA significance $p < 0.05$.

FIGURE 5 Contribution of the Ca^{2+} current and RyR3 to the cytosolic fluorescence determined in RyR1 KO myotubes. Panels *A* and *B* show the maximal confocal Ca^{2+} fluorescence (*A*) and peak Ca^{2+} current (*B*) for nontransfected and β2a-transfected RyR1 KO and RyR1/RyR3 KO myotubes. Cells were depolarized for 200 ms from a holding potential of -40 mV. The mean $\pm$ SE maximal $\Delta F/F$ and Ca^{2+} current are plotted for five nontransfected RyR1 KO myotubes (*open circles*); 7 RyR1 KO myotubes overexpressing β2a (*closed circles*); 3 nontransfected RyR1/RyR3 KO myotubes (*open squares*); and 7 RyR1/RyR3 KO myotubes overexpressing β2a (*closed squares*). The maximal Ca^{2+} fluorescence during the Ca^{2+} transients was obtained from the integrated confocal line scan image as described in Materials and Methods. Panel *C* shows Ca^{2+} transients and Ca^{2+} currents at $+30$ mV in an RyR1 KO myotube overexpressing β2a in external solution (control; *black traces*) and external solution supplemented with five μM ryanodine (*gray traces*). The pulse duration was 200 ms and the holding potential was -40 mV. The digitized traces show fluo-4 fluorescence in $\Delta F/F$ units obtained during the confocal line scan. Each dot corresponds to the mean fluorescence of a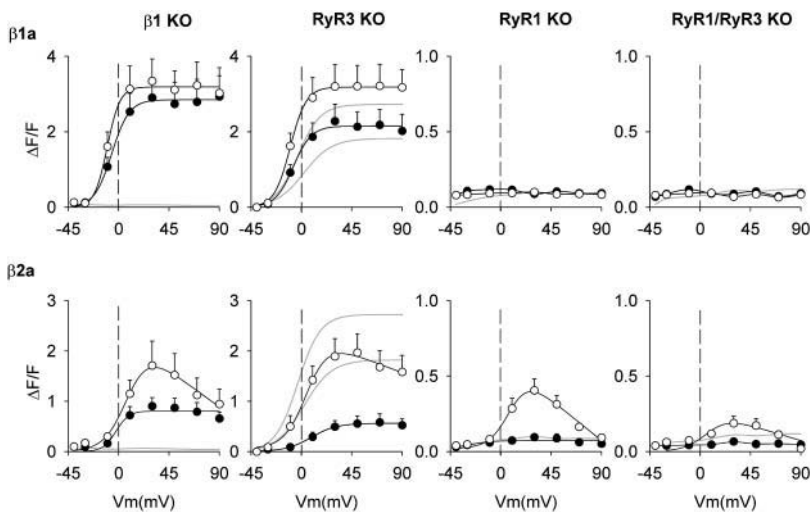 single 512-pixel line acquired at a rate of 2.05 ms per line. Ca^{2+} currents acquired concurrently are shown below traces of fluorescence. Panel *D* shows the maximal fluorescence in $\Delta F/F$ units during a 200-ms stimulus divided by the maximal Ca^{2+} current in the same myotube acquired concurrently. Entries correspond to the mean $\pm$ SE for β2a-expressing β1 KO (0.41 ± 0.11, $n = 10$ cells), RyR3 KO (0.29 ± 0.05, $n = 14$ cells), RyR1 KO (0.08 ± 0.02, $n = 5$ cells), and RyR1/RyR3 KO (0.05 ± 0.01, $n = 7$ cells) myotubes.

component of the fluorescence signal in β2a-expressing RyR1 KO myotubes was due to RyR-dependent SR Ca^{2+} release presumably mediated by RyR3. Since Ca^{2+} current densities in all β2a-expressing genotypes were roughly similar (Table 1), we estimated the relative magnitude of the β2a-mediated Ca^{2+} release in all genotypes by normalizing the peak $\Delta F/F$ relative to the magnitude of the Ca^{2+} current at the same potential of $+30$ mV (Fig. 5 *D*). The normalized signal in RyR1/RyR3 KO myotubes represents the direct contribution of the Ca^{2+} current to the cell fluorescence, and progressively larger signals due to SR Ca^{2+} release were present in RyR1 KO, RyR3 KO, and β1 KO myotubes. The largest Ca^{2+} release signals were observed in the RyR1-expressing myotubes (β1 KO and RyR3 KO) consistent with the idea that RyR1 is expressed at a much higher density than RyR3 described above. Voltage-dependent components in β2a-transfected RyR3 KO and β1 KO myotubes also contributed to the fluorescence signal in these cells and are discussed separately (see Figs. 6 and 9). The cell fluorescence to Ca^{2+} current ratio at $+30$ mV was not statistically different for β2a-transfected RyR3 KO and β1 KO myotubes. However, this ratio was significantly smaller for β2a-transfected RyR1 KO and RyR1/RyR3 KO myotubes (*t*-test significance $p < 0.05$) and is indicated by asterisks. The main conclusions from the comparison in Fig. 5 *D* are that the Ca^{2+} current has a modest impact on the measured myotube fluorescence and that both RyR isoforms (RyR1 and RyR3), when present, can be activated by the Ca^{2+} current recovered by β2a overexpression.

Ca^{2+} release triggered by the Ca^{2+} current follows the voltage dependence of the Ca^{2+} current. Hence, this EC coupling mechanism can be distinguished from purely voltage-dependent EC coupling by the shape of the Ca^{2+} fluorescence versus voltage relationship. Additionally, Ca^{2+}-dependent EC coupling should be a sensitive function of the duration of the depolarizing stimulus as longer depolarizations increase the amount of trigger Ca^{2+} entering the cell. Previous studies showed that depolarizations for 50 ms were adequate for activation of DHPR charge movements (Ahern et al., 2003). However, activation of the Ca^{2+} current to near steady state required depolarizations of 200 ms (Sheridan et al., 2003a). For these reasons, we investigated the shape of fluorescence versus voltage curves for depolarizations of 50 and 200 ms in the same cell. Fluorescence versus voltage relationships are shown in Fig. 6 for β1a and β2a overexpression in the four myotube genotypes under investigation. The $\Delta F/F$ value reached at the end of the depolarization was plotted as a function of voltage for depolarizations of 50 ms (*closed symbols*) and 200 ms (*empty symbols*). The gray traces indicate the mean fluorescence of nontransfected myotubes. The duration of the pulse did not affect the sigmoidal voltage dependence of Ca^{2+} transients expressed by β1a in β1 KO myotubes, which is in agreement with recent observation from our laboratory (Sheridan et al., 2003a) and studies in adult skeletal muscle (Melzer et al., 1986). Interestingly, RyR3 KO myotubes overexpressing β1a had sigmoidal fluorescence versus voltage curves with a higher maximal

FIGURE 6 Sigmoidal and bell-shaped voltage dependence of Ca^{2+} transients in myotubes expressing the heterologous DHPR β2a-subunit. Ca^{2+} transients in $\Delta F/F$ units were measured in myotubes with the indicated phenotype (β1 KO, RyR3 KO, RyR1 KO and double RyR1/RyR3 KO) expressing β1a (*top row*) or β2a (*bottom row*). The depolarization duration was 50 ms (closed symbols) or 200 ms (*open symbols*) from a holding potential of -40 mV. The same myotube was subjected to the 50-ms and 200-ms depolarization protocols. Ca^{2+} transients were measured at the end of each depolarization from the time course of the integrated confocal line scan image fluorescence. The lines correspond to a Boltzmann fit of the population mean $\Delta F/F$ indicated in Table 2. All fluorescence vs. voltage curves were fit with Eq. 1 except those obtained with the 200 ms depolarization in myotubes overexpressing β2a, which were fit with Eq. 2. Parameters of the fitted lines ($\Delta F/F_{max}$ in $\Delta F/F$ units, V1/2 in mV, and k in mV) for β1 KO overexpressing β1a are: 2.8, -6.1, 7.8 for 50 ms and 3.2, -10.2, 5.7 for 200 ms. Parameters for β1 KO overexpressing β2a are: 0.8, -2.5, 5.8 for 50 ms and 1.8, 9, 9.7 for 200 ms. Parameters for RyR3 KO overexpressing β1a are: 2.2, -7.2, 8.2 for 50 ms and 3.2, -9.9, 7.3 for 200 ms. Parameters for RyR3 KO overexpressing β2a are: 0.6, 8.5, 11.3 for 50 ms and 1.5, 3.6, 10 for 200 ms. Parameters for RyR1 KO overexpressing β2a are: 0.4, 9.8, 8.9 for 200 ms. Parameters for RyR1/RyR3 KO overexpressing β2a are: 0.2, 7.9, 10 for 200 ms.

fluorescence ($\Delta F/F_{max}$) for the 200 ms than for the 50 ms stimulation. This difference was also observed in non-transfected myotubes ($\Delta F/F_{max} = 1.8 \pm 0.1$ for 50 ms and 2.7 ± 0.1 for 200 ms for four cells) and is shown by the two gray traces in the top and bottom graphs corresponding to RyR3 KO myotubes. However, the differences in $\Delta F/F_{max}$ for 50-ms and 200-ms depolarizations were not significant either in β1a-transfected (see Table 2) or nontransfected RyR3 KO myotubes. A contribution of RyR3 to the overall rate of propagation of Ca^{2+} release has been previously reported in cultured RyR3 KO myotubes and could underlie the small difference in $\Delta F/F_{max}$ observed here for the short and long depolarizations (Yang et al., 2001). In RyR1 KO and RyR1/RyR3 KO myotubes, β1a overexpression failed to recover Ca^{2+} transients entirely, in agreement with the critical role of RyR1 in voltage-dependent coupling and the absence of β1a stimulated Ca^{2+} current expression in these genotypes. β2a overexpression changed the shape of the fluorescence versus voltage curve in the RyR1-expressing genotypes (β1 KO and RyR3 KO) and introduced Ca^{2+} transients in the RyR1-deficient genotypes (RyR1KO and RyR1/RyR3 KO) that were not present in nontransfected counterparts. In β1 KO and RyR3 KO myotubes, β2a-overexpression reduced the $\Delta F/F_{max}$ produced by the 50-ms stimulation relative to that recovered by β1a, and furthermore, the fluorescence versus voltage curves generated with the 200-ms pulse were clearly bell-shaped. Bell-shaped curves were also observed for the 200-ms depolarization in RyR1 KO and RyR1/RyR3 KO myotubes but not for the 50-ms depolarization. In all cases, the 200-ms depolarization produced an increase in fluorescence in the range of -30 mV to $+20$ mV, a maximum at $\sim +30$ mV, and a decline in fluorescence in the range of $+40$ mV to $+90$ mV. To

quantify these observations, we fitted the curves obtained with the 200-ms depolarization for β2a-expressing myotubes with a modified Boltzmann equation that takes into account the reversal potential of the Ca^{2+} current (Eq. 2), whereas the rest of the curves in Fig. 6 were fit with a conventional Boltzmann equation (Eq. 1). The degree of curvature of the fluorescence versus voltage plots at positive potentials was estimated by computing the ratio of fluorescence at the experimental maximum (*exp max*) for a given fluorescence versus voltage curve (typically $+30$mV) and the fluorescence at $+90$ mV ($[\Delta F/F\,exp\,max]/[\Delta F/F+90\,mV]$). The Boltzmann parameters of the fit of each cell and the fluorescence ratios at 50 ms and 200 ms are shown in Table 2 along with the statistical significance and the number of cells. In summary, a dependence of the Ca^{2+} transient amplitude on pulse duration was observed for β2a-overexpressing myotubes. This was reflected in the bell-shaped fluorescence versus voltage relationships, consistent with the presence of an EC coupling component triggered by the Ca^{2+} current in all myotube genotypes overexpressing β2a. Ca^{2+} transients were the smallest in RyR1/RyR3 KO myotubes, and, as mentioned previously, they reflected the fluorescence contributed by the Ca^{2+} current itself.

If the Ca^{2+} current triggered SR Ca^{2+} release in myotubes expressing β2a, the rate of rise of the fluorescence signal and the rate of Ca^{2+} entering the cell should have a similar time course. Fig. 7 shows Ca^{2+} transients and Ca^{2+} currents produced by a 200-ms depolarization to $+30$ mV from a holding potential of -40 mV in the four myotube genotypes. To correlate the time course of the Ca^{2+} transient and the Ca^{2+} current, we compared the cumulative sum of the Ca^{2+} entry charge during the depolarization (i.e., the running integral of the Ca^{2+} current) with the fluorescence
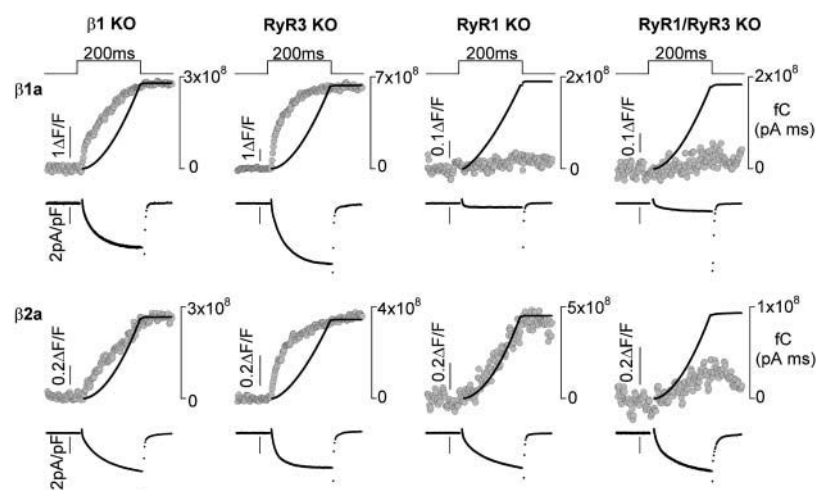
FIGURE 7 Correlation between the rate of cytosolic Ca^{2+} increase and rate of Ca^{2+} accumulation in myotubes overexpressing the heterologous DHPR $\beta 2a$-subunit. Each panel shows Ca^{2+} currents and Ca^{2+} transients in myotubes of the indicated genotype ($\beta 1$ KO, RyR3 KO, RyR1 KO, and double RyR1/RyR3 KO) overexpressing $\beta 1a$ (*top row*) or $\beta 2a$ (*bottom row*) in response to a 200-ms depolarization from a holding potential of –40 mV to +30 mV in external solution with 10 mM Ca^{2+}. The digitized trace (*gray*) shows fluo-4 fluorescence in $\Delta F/F$ units during the confocal line scan. Each dot corresponds to the mean fluorescence of a single 512-pixel line acquired at a rate of 2.05 ms per line. The black trace shows the cumulative integral of the Ca^{2+} current (running integral) in *fC* (pA × ms) superimposed on the fluorescence trace. Actual Ca^{2+} currents are shown below the trace of fluorescence. Note changes in $\Delta F/F$ units and *fC* units.

signal. We have previously argued that this is a fair comparison because Ca^{2+} fluorescence was measured in an internal solution containing a low EGTA concentration (0.1 mM), and, thus, the cell fluorescence tracked Ca^{2+} accumulation rather than the rate of SR Ca^{2+} release (Sheridan et al., 2003a,b). Accordingly, the confocal fluorescence every 2.05 ms (*gray dots* in $\Delta F/F$ units), and the running integral of the Ca^{2+} current (*smooth curve* in *black* in units of pA × ms) were superimposed. For the RyR1-expressing myotubes ($\beta 1$ KO and RyR3 KO) with $\beta 1a$-overexpression, the fluorescence signal increased earlier and faster than the Ca^{2+} charge. Furthermore, the fluorescence signal saturated before termination of the 200-ms pulse, whereas the Ca^{2+} charge continued to increase for as long as the pulse was at +30 mV. In contrast, Ca^{2+} transients obtained by $\beta 2a$-overexpression were considerably slower than those obtained by $\beta 1a$-overexpression. Furthermore, there was a much closer agreement in the kinetics of the two signals in myotubes overexpressing $\beta 2a$, which was particularly compelling in the $\beta 2a$-expressing RyR1 KO myotube. In RyR1/RyR3 KO myotubes, the fluorescence signal was too noisy to permit a comparison, and, for that reason, it was not expanded. In summary, $\beta 2a$ overexpression eliminated the fast EC coupling typical of skeletal myotubes. Furthermore, the slow EC coupling observed in myotubes expressing $\beta 2a$ appears to have its kinetic basis on the slow time course of the skeletal DHPR Ca^{2+} current.

In the RyR1-expressing $\beta 1$ KO and RyR3 KO myotubes, it could be argued that $\beta 2a$ induced a mixed form of EC coupling with voltage and Ca^{2+} serving as triggers. This is based on the fact that a pool of native DHPRs is expected to be present in these cells even after $\beta 2a$-overexpression. In addition, in $\beta 1$ KO and RyR3 KO myotubes overexpressing $\beta 2a$, the 50-ms depolarization produced $\Delta F/F$ versus voltage curves with a quasi-sigmoidal shape, whereas the 200-ms depolarization induced relationships that were clearly bell-

shaped (Fig. 6). Thus, the brief depolarization may not have been sufficient to fully activate the slow Ca^{2+} current but may have been sufficient to activate DHPR voltage sensors and trigger voltage-dependent EC coupling. To demonstrate if mixed voltage and Ca^{2+} dependent coupling had occurred, Ca^{2+} transients were measured in $\beta 2a$-expressing $\beta 1$ KO, RyR3 KO, and RyR1 KO myotubes before and after inhibition of the Ca^{2+} current with 2.5 μM nifedipine. Fig. 8 shows Ca^{2+} currents in the same myotube in response to a depolarization to +30 mV from a holding potential of –40 mV. In these experiments, we used $\beta 1a$-overexpressing $\beta 1$ KO myotubes as a control since this isoform fully restores skeletal-type EC coupling (Beurg et al., 1997; Sheridan et al., 2003a). In all cases, fast-perfusion with external solution containing nifedipine abolished the Ca^{2+} current to a level below detection (*gray traces*), which was ~20 pA/cell. Ca^{2+} transients monitored concurrently are shown before and after Ca^{2+} current inhibition. In the $\beta 1$ KO myotubes overexpressing $\beta 1a$, approximately half of the Ca^{2+} transient was resistant to nifedipine, consistent with previous studies in cultured skeletal myotubes (Nakai et al., 1998a; Wilkens et al., 2001). The partial inhibitory effect of nifedipine on skeletal-type EC coupling has been previously documented and is presumably due to partial inhibition of DHPR charge movements (Rios and Pizarro, 1991). Similarly, nifedipine produced a partial block of Ca^{2+} transients in RyR3 KO myotubes, consistent with the idea of mixed voltage and Ca^{2+} dependent coupling in this genotype. In contrast, nifedipine treatment entirely eliminated Ca^{2+} transients induced by $\beta 2a$ overexpression in $\beta 1$ KO and RyR1 KO myotubes. Hence, in these cells, the Ca^{2+} current was overwhelmingly responsible for triggering EC coupling. In a few $\beta 2a$-expressing $\beta 1$ KO cells, we observed a small nifedipine-insensitive fluorescence signal, which could be attributed to a minor component of skeletal-type EC coupling promoted by $\beta 2a$. However, this was not consistently observed in all batches of transfected cells, pre-
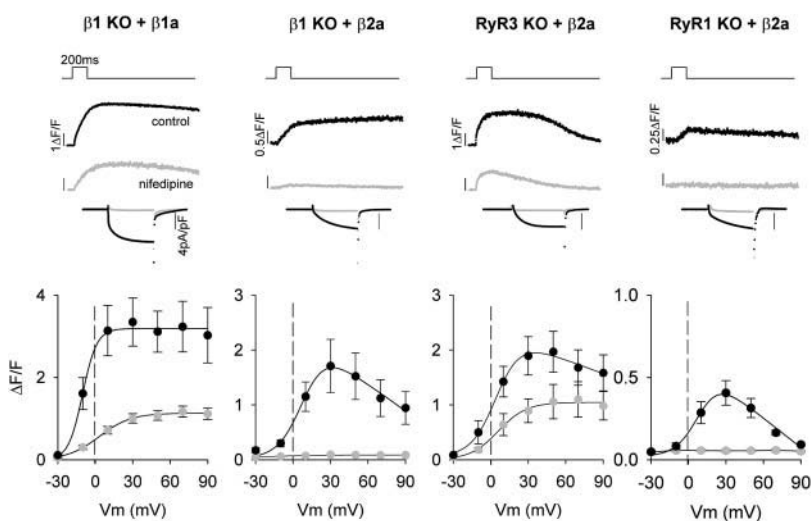
FIGURE 8 Nifedipine-sensitive Ca^{2+} transients expressed by the heterologous DHPR β2a-subunit in β1 KO, RyR3 KO, and RyR1 KO myotubes. From left to right, the panels show Ca^{2+} transients, Ca^{2+} currents, and fluorescence versus voltage curves for β1a in β1 KO, β2a in β1 KO, β2a in RyR3 KO, and β2a in RyR1 KO myotubes. Myotubes were depolarized for 200 ms from a holding potential of -40 mV to $+30$ mV in external solution with 10 mM Ca^{2+}. Ca^{2+} transients and Ca^{2+} currents were measured in the same myotube before and after block of the Ca^{2+} current with 2.5 μM nifedipine. Time course of the Ca^{2+} transient and Ca^{2+} current after nifedipine inhibition is shown in gray. The time course of the cell fluorescence was obtained by integration of the line scan image as described in Materials and Methods. Graphs show the fit of voltage dependence of the maximal $\Delta F/F$ during the depolarization using Eq. 1 for β1a overexpression or Eq. 2. for β2a overexpression. Gray symbols show fluorescence versus voltage curve after myotube exposure to nifedipine.

sumably due to the small magnitude of the signal and the variability in the levels of the expressed protein. In summary, the pharmacological approach indicated that a mixed form of EC coupling was observed in RyR3 KO myotubes. However, the Ca^{2+} current appeared to be more important than voltage as EC coupling trigger in β1 KO and RyR1 KO myotubes overexpressing β2a.

The pharmacological approach using nifedipine indicated that β2a overexpression promoted Ca^{2+}-dependent EC coupling. However, the loss of voltage-dependent EC coupling could not be directly determined since nifedipine partially inhibited voltage sensors. To determine the extent to which voltage-dependent EC coupling was reduced by β2a overexpression, we coexpressed β2a and a Ca^{2+}-impermeant α1S pore mutant (E1014K) in a double dysgenic/β1 KO myotube lacking WT α1S- and β1a-subunits. Previous studies in dysgenic (α1S-null) myotubes had shown that substitution of a critical glutamate residue at position 1014 by lysine in the pore loop of repeat III of α1S completely abolished inward Ca^{2+} currents, whereas skeletal-type EC coupling was restored quantitatively (Dirksen and Beam, 1999; Ahern et al., 2001b). Thus, by coexpressing β2a and the nonconducting α1S-subunit in a null background for both subunits, we assessed voltage-dependent EC coupling promoted directly by β2a in the absence of Ca^{2+} current trigger. Double mutant mice lacking α1S and β1a were obtained by interbreeding dysgenic and β1 KO mice heterozygous for the *mdg* and β1 KO alleles as described in Materials and Methods. Similar to dysgenic and β1 KO myotubes, double dysgenic/β1 KO myotubes were previously shown to be entirely devoid of Ca^{2+} currents and EC coupling. Furthermore, only by coexpressing both missing subunits in double dysgenic/β1 KO myotubes (α1S + β1a), was the normal skeletal myotube phenotype restored (Ahern et al., 1999). To form the α1S/β1a and α1S/β2a subunit pairs, the β variant cDNAs were transfected in β1 KO

myotubes which are otherwise WT for α1S and the other DHPR genes (Gregg et al., 1996). To form the α1S (E1014K)/β1a pair, the mutant α1S (E1014K) cDNA was transfected in dysgenic myotubes which are otherwise WT for β1 and other DHPR genes (Chaudhari, 1992; Ahern et al., 1999; Arikkath et al., 2003). Fig. 9 shows Ca^{2+} transients and Ca^{2+} currents at $+30$ mV from a holding potential of -40 mV in response to a 200-ms depolarization in three myotube genotypes under the same conditions. Panel *A* shows a β1 KO myotube expressing β1a and separately a dysgenic myotube expressing α1S (E1014K). Panel *C* shows a β1 KO myotube expressing β2a and separately a double dysgenic/β1 KO myotube coexpressing α1S (E1014K) + β2a. Average fluorescence versus voltage and current versus voltage curves are shown in panels *B* and *D*, respectively. At $+30$ mV, the maximal Ca^{2+} current densities were -5.4 ± 0.3 pA/pF (10 cells) and -4.6 ± 0.7 (10 cells) for myotubes expressing the WT α1S/β1a and WT α1S/β2a pairs, respectively, in panels *B* and *D*. In contrast, the pore mutant inward currents at the same potential were below the level of detection (~0.05 pA/pF), in agreement with previous results (Dirksen and Beam, 1999; Ahern et al., 2001b). Outward currents at potentials more positive than $+30$ mV correspond to a mixture of background currents present in the cultured myotube and outward monovalent current through the pore mutant Ca^{2+} channel (Yang et al., 1993).

As indicated by the average $\Delta F/F$ curves in Fig. 9 *B*, Ca^{2+} transients of a comparable maximal magnitude and sigmoidal voltage dependence were obtained in β1 KO myotubes expressing β1a and dysgenic (labeled *mdg*) myotubes expressing α1S (E1014K). Thus, expressed DHPRs carrying either a WT or a pore-mutant α1S-subunit were capable of restoring voltage-dependent EC coupling. This result is in accordance with the well-known lack of involvement of the L-type Ca^{2+} current as EC coupling trigger in skeletal
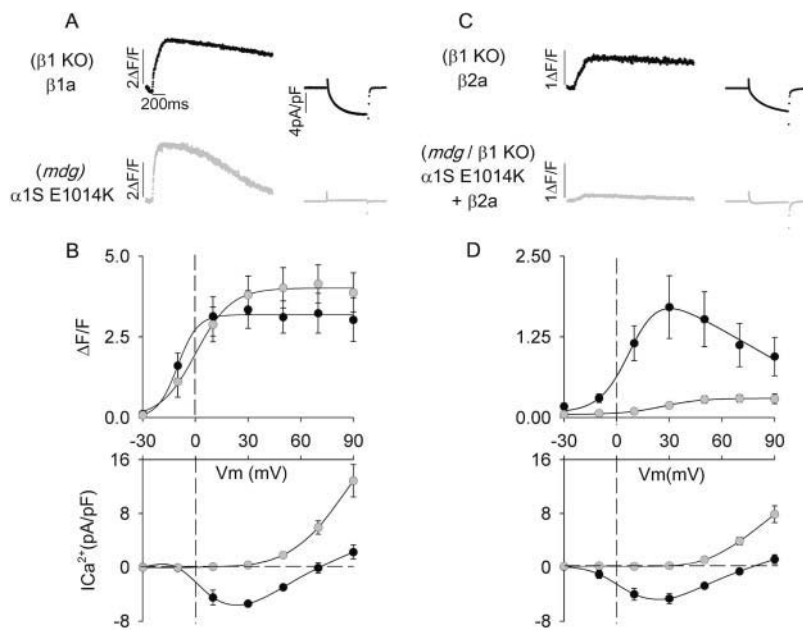
FIGURE 9 Ca^{2+} transients and Ca^{2+} currents expressed by the heterologous DHPR β2a-subunit in α1S/β1-null myotubes. Ca^{2+} transients and Ca^{2+} currents in the same myotube at $+30$ mV from a holding potential of -40 mV in response to a 200-ms depolarization. Panel A shows a β1 KO myotube transfected with β1a (*black traces*) and a dysgenic myotube (labeled *mdg*) transfected with α1S (E1014K) (*gray traces*). Panel B shows average fluorescence versus voltage and current versus voltage curves for β1 KO myotubes expressing β1a (*black traces*) and dysgenic myotubes expressing α1S (E1014K) (*gray traces*). Fluorescence and whole cell current data are shown for 10 and 5 cells in black and gray symbols, respectively. Panel C shows a β1 KO myotube transfected with β2a (*black traces*) and a double dysgenic /β1 KO myotube cotransfected with β2a and α1S (E1014K) (*gray traces*). Panel D shows average fluorescence versus voltage and current versus voltage curves for β1 KO myotubes expressing β2a (*black traces*) and for double dysgenic/β1 KO myotubes coexpressing β2a + α1S (E1014K) (*gray traces*). Fluorescence and whole cell current data are shown for 10 and 8 cells in black and gray symbols, respectively. Parameters of the Boltzmann fit of fluorescence were $\Delta F/F_{max}$ in $\Delta F/F$ units, V1/2 in mV, and k in mV) were 4 ± 0.6, 1 ± 6, 8 ± 1.1 (α1S (E1014K), 5 cells) and 0.3 ± 0.1, 24 ± 5, 9.3 ± 1.3 (β2a + α1S (E1014K), 8 cells). Parameters for β1a and β2a expressing cells in β1 KO myotubes are shown in Table 2.

muscle and, more specifically, with the behavior of α1S (E1014K) in previous studies in dysgenic myotubes (Dirksen and Beam, 1999; Ahern et al., 2001b). In contrast, Ca^{2+} transients in double dysgenic/β1 KO myotubes expressing α1S (E1014K) and β2a in Fig. 9 D were substantially smaller than those in β2a-expressing β1 KO myotubes. Thus, elimination of the pore function in the α1S-subunit curtailed the magnitude of the Ca^{2+} transient when β2a formed part of the DHPR complex. Moreover, the fluorescence versus voltage curve was bell-shaped in the case of the WT α1S/β2a pair but sigmoidal for the α1S (E1014K)/β2a pair, consistent with the idea that the pore mutant DHPR contributed only to voltage-dependent EC coupling. The bell-shaped fluorescence versus voltage curve for the WT α1S/β2a pair was in agreement with data in Fig. 6. From the magnitude of Ca^{2+} transients in β2a-expressing β1 KO myotubes and α1S (E1014K) + β2a-expressing double dysgenic/β1 KO myotubes in Fig. 9 D, we estimated that the voltage-dependent component of EC coupling was ~20% of the total Ca^{2+} transient at $+30$ mV. From these observations we concluded that the DHPR β2a-subunit eliminated a sizable amount of voltage-dependent EC coupling despite the presence of a WT α1S pore subunit. Hence, in myotubes overexpressing β2a and lacking β1a, Ca^{2+} entry dominates over voltage as EC coupling trigger.

DISCUSSION

This work shows that replacement of the skeletal DHPR β1a-subunit by the cardiac/brain variant β2a, in the context

of a WT α1S pore subunit, modifies the EC coupling signal from one controlled by voltage to one controlled by the Ca^{2+} current. The changes in EC coupling were most pronounced in β1 KO myotubes and, by comparison to β1a, β2a produced an overall decrease in the amplitude of Ca^{2+} transients with evident changes in the shape of the Ca^{2+} fluorescence versus voltage relationship, slowing of the kinetics of the Ca^{2+} transient, and a dependence of Ca^{2+} transients on the Ca^{2+} current. These observations, the pharmacological interventions using nifedipine, and the results in double dysgenic/β1 KO myotubes are all consistent with a loss in voltage-dependent EC coupling and emergence of Ca^{2+}-dependent EC coupling triggered by the slow L-type DHPR Ca^{2+} current. Partial changes in the same direction were also observed when β2a was overexpressed in the presence of a native skeletal DHPR, such as in RyR3 KO myotubes. In this case, β2a appeared to have acted as a negative dominant which is presumably due to the inability of the functional hybrid DHPR composed of skeletal subunits and β2a to fully engage in skeletal-type EC coupling. Overall, the changes promoted by the β2a-subunit are mechanistically important since, until this work, only cardiac/brain DHPR α1 pore subunits (Garcia et al., 1994; Nakai et al., 1998a), were known to introduce Ca^{2+}-dependent EC coupling in skeletal myotubes.

By comparing $\Delta F/F_{max}$ for the α1S (E1014K)/β1a and α1S (E1014K)/β2a subunit pairs we can roughly estimate the loss in skeletal-type EC coupling when β1a is replaced by β2a in the DHPR complex. $\Delta F/F_{max}$ was 4 ± 0.6 (5 cells) and 0.3 ± 0.1 (8 cells), respectively. Hence, voltage

was ~10-fold less effective as a trigger signal when the skeletal DHPR included the cardiac/brain β2a isoform as a β-subunit. This occurred despite the fact that Ca^{2+} current densities and previously estimated single-channel open probabilities were similar when β2a replaced β1a in the context of a WT α1S pore subunit (Beurg et al., 1999b). Thus, DHPR densities were likely to be similar when either β1a or β2a formed part of the DHPR complex. Based on the small magnitude of the voltage-dependent component, we would have predicted stronger differences in Ca^{2+} transient amplitudes in β2a-expressing myotubes for 50-ms and 200-ms depolarizations since the brief depolarization injects between 5-fold and 130-fold less Ca^{2+} charge into the cell depending on channel kinetics (Sheridan et al., 2003a). Instead, Fig. 6 shows only a twofold difference in Ca^{2+} transient fluorescence at +30 mV for 50 ms and 200 ms in β2a-transfected β1 KO myotubes. It is entirely possible that a voltage-activated Ca^{2+} release component, even if small, may lead to an explosive activation of near-neighbor RyRs by a Ca^{2+}-dependent mechanism. Hence the comparatively large activation of Ca^{2+} release seen at 50 ms may not reflect the magnitude of the voltage-dependent component. Rather, it may reflect the effect of the voltage-dependent component on a much larger population of RyR channels, most of them activated by Ca^{2+} released from a few voltage-activated RyRs. Such a mechanism has been suggested for Ca^{2+} spark formation in frog skeletal and cardiac muscle. However, its applicability to mammalian skeletal muscle still is under investigation (Stern et al., 1997). It is also possible that the absence of normal interaction between the DHPR and RyR1 when β2a is present renders RyR1 more Ca^{2+}-sensitive such that smaller Ca^{2+} currents may recruit a larger density of Ca^{2+}-activated RyR channels. Both possibilities suggest synergistic interactions between voltage and Ca^{2+} as trigger signals which remain to be investigated in more detail.

The observed loss of voltage-dependent and gain of Ca^{2+}-dependent EC coupling, in the context of a WT α1S-subunit, implies a change in the mechanism of interaction of the DHPR and RyR1. Structural studies have shown that, at transverse tubular-SR junctions, four DHPRs arranged as a square tetrad hover over the cytoplasmic surface of a single RyR1 tetramer (reviewed by Franzini-Armstrong and Protasi, 1997). This anatomical arrangement, and the minimal distance separating the SR and surface-connected membranes at these locations, has provided compelling evidence in favor of a protein-to-protein "mechanical-type" coupling between the skeletal DHPR and RyR1. The EC coupling signal transferred from the voltage sensor to RyR1 may thus involve some form of mechanical torque exerted on the foot structure of RyR1 initiated by voltage sensor movement. The essence of this concept was originally proposed by Chandler et al. (1976), although the nature of the protein complexes involved in voltage sensing and SR Ca^{2+} release were not known at the time. In this context, the

EC coupling changes promoted by β2a-subunit are most easily visualized as a partial undocking of the DHPR and RyR1 complexes. Ca^{2+}-dependent EC coupling might thus result from a partially-docked DHPR-RyR1 complex in which the voltage signal is unable to open a significant number of RyR1 channels. Those RyR1 channels not activated by voltage might be available for activation by the Ca^{2+} current provided that the DHPR and the RyR1 remain co-localized. It could be further argued that in normal circumstances, the Ca^{2+} current has no impact on EC coupling because during a brief depolarization, and before the full activation of the Ca^{2+} current, the complete pool of RyR channels in a given release unit is rapidly and synchronically activated. Some of the RyR1 channels would be directly activated by voltage via "mechanical" coupling to the DHPR and others would be activated by the Ca^{2+} released from the nearest voltage-activated RyR1 channel. Rapid and synchronic activation of voltage-dependent and Ca^{2+}-dependent RyR channels has been proposed to occur during Ca^{2+} spark formation in adult skeletal muscle (Stern et al., 1997).

Expression of the native DHPR Ca^{2+} current appears to be under the specific control of RyR1 by a so-called retrograde signal from RyR1 to the DHPR. This retrograde signal is probably structural in origin since a WT Ca^{2+} current density was observed in RyR1 KO myotubes expressing RyR1 mutants deficient in EC coupling (Avila et al., 2001). Recent studies showed that the requirement of the DHPR for RyR1 could be bypassed by molecular determinants present on the amino terminus of β2a (Ahern et al., 2003). Ca^{2+} currents were present at a WT density in RyR1 KO myotubes overexpressing β2a or β2a-β1a chimeras carrying domains D1, D2, and D3 of β2a (Ahern et al., 2003). Two vicinal cysteines in domain D1, a putative palmitoylation motif, were critical for the β2a-mediated Ca^{2+} current recovery. Furthermore, tethering β2a to the myotube surface by a transmembrane motif in the absence of the two vicinal cysteines in domain D1 also increased Ca^{2+} current expression in the absence of RyR1. Thus, the conformational state of the β-subunit, or preferential locations of the β-subunit close to the plasma membrane, are crucial for DHPR Ca^{2+} current expression. In the native DHPR, such a specific conformation of the β-subunit may be reached through a direct interaction with RyR1 (Cheng and Coronado, 2003). However, we realize that Ca^{2+} current regulation in the skeletal DHPR is quite complex and that it involves molecular determinants present in α1S (Grabner et al., 1999), RyR1 (Nakai et al., 1998b), as well as in the β-subunit (Ahern et al., 2003). Even though the mechanism for Ca^{2+} current enhancement by β2a has been outlined, it could still be argued that β2a either recruited other pore subunits in the culture myotube and/or redirected the DHPR to surface locations away from EC coupling sites. Functional evidence gathered previously (Ahern et al., 2003; Sheridan et al., 2003a) and in this work, indicates that both possibilities are

unlikely. As already mentioned, transfection of β1a in a dysgenic α1S-null myotube does not result in expression of Ca^{2+} currents (not shown). Therefore, non-α1S pore subunits that could account for Ca^{2+} current recovery by β2a are not present in the cultured myotube. Furthermore, we could not detect significant differences in the skeletal-type EC coupling abilities of β2a-β1a chimeras with and without the double cysteine motif, provided that the carboxyl terminus of β1a was present (Ahern et al., 2003). This result argues that the double cysteine motif does not have an intrinsic ability to relocate the DHPR to new sites in the myotube surface away from the junctional SR region. These reasons, and the fact that Ca^{2+}-dependent release was observed, altogether, make it likely that hybrid DHPRs that include α1S and β2a are present at SR junctions but are not strongly docked to RyR1. Strong co-localization is a condition sine qua non for observing Ca^{2+}-dependent release since other high-density Ca^{2+} currents in the myotube such as those originating from T-type Ca^{2+} channels do not release SR Ca^{2+} (Ahern et al., 2001d).

This work implicates RyR3 in SR Ca^{2+} release in cultured skeletal myotubes. RyR3 is widely expressed in fetal limb muscles, abdominal muscles, and in the diaphragm (Bertocchini et al., 1997). During the neonatal phase, RyR3 expression is drastically reduced, whereas in the adult musculature, this isoform is almost exclusively confined to the diaphragm and soleus muscles (Bertocchini et al., 1997; Flucher et al., 1999). Hence, the presence of RyR3 in cultured myotubes derived from limb fetal tissue is not surprising, and our observation is in agreement with a previous report (Takeshima et al., 1995). In β1a-over-expressing and nontransfected RyR3 KO myotubes, the 200-ms depolarization evoked more release, i.e., a higher $\Delta F/F_{max}$, than the shorter 50-ms depolarization. This behavior was not present in either WT or β1a-expressing β1 KO myotubes (Table 1). RyR3 is known to form functional Ca^{2+} release units, as demonstrated by its ability to generate spontaneous Ca^{2+} spark-like Ca^{2+} release events in several expression systems (Conklin et al., 2000; Ward et al., 2000; Rossi et al., 2002). Furthermore, RyR3 is present in transverse tubular-SR junctions (Flucher et al., 1999) and contributes substantially to the kinetics and overall dimensions of Ca^{2+} sparks in WT muscle cells (Conklin et al., 2000). In cultured myotubes, Ca^{2+} release sites are present in peripheral couplings established between junctional SR and surface membranes (Takekura et al., 1994). Confocal studies in cultured myotubes have shown that the rate of SR Ca^{2+} release propagation from the edge to the center of the cell is considerably slower in RyR3 KO than in RyR3-expressing controls. Thus, a significant functional role of RyR3 channels is to synchronize the macroscopic Ca^{2+} release transient in different regions of the myotube (Yang et al., 2001). Our findings are consistent with this observation, since a brief depolarization is expected to be less effective than a longer depolarization in speeding inward Ca^{2+} release

propagation. In our data, this would be manifested as a decrease in the space-averaged fluorescence. It is interesting to note that a decrease in space-averaged Ca^{2+} fluorescence is also evident in the line scan images in Fig. 1 B of Yang et al. (2001) comparing RyR3-deficient and RyR3-expressing myotubes, although calculations were not reported. Mammalian RyR3 channels have a mean open time much longer than RyR1 channels (Chen et al., 1997) and a lower sensitivity to inactivation by Ca^{2+} (Sonnleitner et al., 1998) and Mg^{2+} (Murayama and Ogawa, 1997). We would speculate that during a Ca^{2+} transient, RyR3 channels remain open for longer periods than RyR1 channels. The overall result would be a local positive reinforcement of Ca^{2+} release, and this could be the basis for the enhancement in Ca^{2+} fluorescence observed with the 200-ms depolarization. Our observations in RyR1 KO myotubes further indicate that RyR3 is capable of engaging in Ca^{2+} release triggered directly by the Ca^{2+} current. Hence, RyR3 may not only amplify Ca^{2+} release initiated by RyR1, but, in addition, RyR3 may be a recipient of a bona fide Ca^{2+} current trigger signal.

The changes in the EC coupling trigger signal, from voltage to Ca^{2+} entry, promoted by β2a in β1 KO myotubes, are entirely analogous to the changes in EC coupling observed previously when α1S was replaced by the cardiac α1C-subunit in the cellular context of a primary dysgenic α1S-null skeletal myotube (Tanabe et al., 1990; Garcia et al., 1994). The functional analogy extends also to Ca^{2+} current regulation since α1C, like β2a, expresses high-density Ca^{2+} currents in RyR1 KO myotubes (Carbonneau et al., 2003; unpublished). Hence, Ca^{2+} current expression in a DHPR that includes α1C is not functionally inhibited by the absence of RyR1. The similar outcome of these two sets of experiments, namely α1S replacement by α1C versus β1a replacement by β2a, suggests to us that in the native DHPR, critical interactions with RyR1 responsible for orthograde and retrograde coupling are controlled by conformational states in both α1S and the β-subunit. Hence, we would suggest that the α1S/β pair, and not each subunit alone, controls the EC coupling signal in skeletal myotubes. Whether the role of the β-subunit is to facilitate DHPR-RyR1 docking, i.e., a structural role, or is directly involved in the transmission of the molecular signal to RyR1, is currently under investigation. Both possibilities are suggested by mutagenesis experiments in which deletion of EC domains present in the α1S II-III loop did not entirely abolish voltage-dependent Ca^{2+} transients (Ahern et al., 2001b) and by the fact that β1a binds directly to RyR1 (Cheng and Coronado, 2003).

REFERENCES

Ahern, C. A., J. Arikkath, P. Vallejo, C. A. Gurnett, P. A. Powers, K. P. Campbell, and R. Coronado. 2001a. Intramembrane charge movements and excitation-contraction coupling expressed by two-domain fragments of the Ca^{2+} channel. *Proc. Natl. Acad. Sci. USA*. 98:6935–6940.

Ahern, C. A., D. Bhattacharya, L. Mortenson, and R. Coronado. 2001b. A component of excitation-contraction coupling triggered in the absence of the T671–L690 and L720–Q765 regions of the II–III loop of the dihydropyridine receptor α1S pore subunit. *Biophys. J.* 81:3294–3307.

Ahern, C. A., P. A. Powers, G. H. Biddlecome, L. Roethe, P. Vallejo, L. Mortenson, C. Strube, K. P. Campbell, R. Coronado, and R. G. Gregg. 2001c. Modulation of Ca^{2+} current but not activation of Ca^{2+} release by the gamma 1 subunit of the dihydropyridine receptor of skeletal muscle. *BiomedCentral Physiol.* 1:8. (http://www.biomedcentral.com/1472-6793/1/8).

Ahern, C., P. A. Powers, R. Gregg, and R. Coronado. 1999. Expression of cardiac DHPR α1C in α1$^{-/-}$/β1$^{-/-}$ double mutant skeletal muscle myotubes. *Biophys. J.* 76:467a.

Ahern, C. A., D. C. Sheridan, W. Cheng, L. Mortenson, P. D. Allen, and R. Coronado. 2003. Ca^{2+}current and charge movements in skeletal myotubes promoted by the beta-subunit of the dihydropyridine receptor in the absence of ryanodine receptor type 1. *Biophys. J.* 84:942–959.

Ahern, C. A., P. Vallejo, L. Mortenson, and R. Coronado. 2001d. Analysis of a frame-shift mutant of the dihydropyridine receptor pore subunit (α1S) expressing two complementary protein fragments. *BiomedCentral Physiol.* 1:15. (http://www.biomedcentral.com/1472-6793/1/15).

Arikkath, J., C. C. Chen, C. A. Ahern, V. Allamand, J. D. Flanagan, R. Coronado, R. G. Gregg, and K. P. Campbell. 2003. Gamma 1 subunit interactions within the skeletal muscle L-type voltage-gated calcium channel. *J. Biol. Chem.* 278:1212–1219.

Avila, G., and R. T. Dirksen. 2000. Functional impact of the ryanodine receptor on the skeletal muscle L-type Ca^{2+} channel. *J. Gen. Physiol.* 115:467–479.

Avila, G., K. M. S. O'Connell, L. A. Groom, and R. T. Dirksen. 2001. Ca^{2+} release through ryanodine receptors regulates skeletal muscle L-type Ca^{2+} channel expression. *J. Biol. Chem.* 276:17732–17738.

Barone, V., F. Bertocchini, R. Bottinelli, F. Protasi, P. D. Allen, C. Franzini Armstrong, C. Reggiani, and V. Sorrentino. 1998. Contractile impairment and structural alterations of skeletal muscles from knockout mice lacking type 1 and type 3 ryanodine receptors. *FEBS Lett.* 422:160–164.

Berrou, L., G. Bernatchez, and L. Parent. 2001. Molecular determinants of inactivation within the I–II linker of alpha1E (CaV2.3) calcium channels. *Biophys. J.* 80:215–228.

Bers, D. M. 2002. Cardiac excitation-contraction coupling. *Nature.* 415:198–205.

Bertocchini, F., C. E. Ovitt, A. Conti, V. Barone, H. R. Scholer, R. Bottinelli, C. Reggiani, and V. Sorrentino. 1997. Requirement for the ryanodine receptor type 3 for efficient contraction in neonatal skeletal muscles. *EMBO J.* 16:6956–6963.

Beuckelmann, D. J., and W. G. Wier. 1988. Mechanism of release of calcium from sarcoplasmic reticulum of guinea-pig cardiac cells. *J. Physiol.* 405:233–255.

Beurg, M., C. A. Ahern, P. Vallejo, M. Conklin, P. A. Powers, R. G. Gregg, and R. Coronado. 1999a. Involvement of the carboxy-terminus region of the dihydropyridine receptor beta 1a subunit in excitation-contraction coupling of skeletal muscle. *Biophys. J.* 77:2953–2967.

Beurg, M., M. Sukhareva, C. A. Ahern, M. W. Conklin, E. Perez-Reyes, P. A. Powers, R. G. Gregg, and R. Coronado. 1999b. Differential regulation of skeletal muscle L-type Ca^{2+} current and excitation-contraction coupling by the dihydropyridine receptor beta subunit. *Biophys. J.* 76:1744–1756.

Beurg, M., M. Sukhareva, C. Strube, P. A. Powers, R. G. Gregg, and R. Coronado. 1997. Recovery of Ca^{2+} current, charge movements, and Ca^{2+} transients in myotubes deficient in dihydropyridine receptor beta 1 subunit transfected with beta 1 cDNA. *Biophys. J.* 73:807–818.

Bezanilla, F. 2000. The voltage sensor in voltage-dependent ion channels. *Physiol. Rev.* 80:555–592.

Bichet, D., V. Cornet, S. Geib, E. Carlier, S. Volsen, T. Hoshi, Y. Mori, and M. De Waard. 2000. The I–II loop of the Ca^{2+} channel alpha1 subunit contains an endoplasmic reticulum retention signal antagonized by the beta subunit. *Neuron.* 25:177–190.

Carbonneau, L., D. Bhattacharya, and R. Coronado. 2003. Two beta subunits (beta 1a and beta 3) interact with the cardiac alpha1C pore isoform (Cav 1.2) in skeletal myotubes. *Biophys. J.* 84:262a.

Chandler, W. K., R. F. Raowski, and M. F. Schneider. 1976. Effects of glycerol treatment and maintained depolarization on charge movement in skeletal muscle. *J. Physiol.* 254:285–316.

Chaudhari, N. 1992. A single nucleotide deletion in the skeletal muscle-specific calcium channel transcript of muscular dysgenesis. *J. Biol. Chem.* 267:25636–25639.

Chen, S. R. W., X. Li, K. Ebisawa, and L. Zhang. 1997. Functional characterization of the recombinant type 3 Ca^{2+} release channel (ryanodine receptor) expressed in HEK292 cells. *J. Biol. Chem.* 272:24234–24246.

Cheng, W., and R. Coronado. 2003. Direct binding of skeletal muscle dihydropyridine receptor beta subunit to ryanodine receptor type 1. *Biophys. J.* 84:109a.

Chien, A. J., X. L. Zhao, R. E. Shirokov, T. S. Puri, C. F. Chang, K. Sun, E. Rios, and M. M. Hosey. 1995. Roles of a membrane-localized beta subunit in the formation and targeting of functional L-type Ca^{2+} channels. *J. Biol. Chem.* 270:30036–30044.

Conklin, M., C. A. Ahern, P. Vallejo, V. Sorrentino, H. Takeshima, and R. Coronado. 2000. Comparison of Ca^{2+} sparks produced independently by two ryanodine receptor isoforms (type-1 or type-3). *Biophys. J.* 78:1777–1785.

Conklin, M. W., P. A. Powers, R. G. Gregg, and R. Coronado. 1999. Ca^{2+} sparks in embryonic mouse skeletal muscle selectively deficient in dihydropyridine receptor alpha1S or beta1a subunits. *Biophys. J.* 76:657–669.

Coronado, R., J. Morrissette, M. Sukhareva, and D. M. Vaughan. 1994. Invited Review: Structure and function of ryanodine receptors. *Am. J. Physiol. (Cell Physiol.).* 35:C1485–C1504.

De Waard, M., M. Pragnell, and K. P. Campbell. 1994. Ca^{2+} channel regulation by a conserved beta subunit domain. *Neuron.* 13:495–503.

Dietze, B. F., F. Bertocchini, V. Barone, A. Struk, V. Sorrentino, and W. Melzer. 1998. Voltage-controlled Ca^{2+} release in normal and ryanodine receptor type 3 (RyR3)-deficient mouse myotubes. *J. Physiol.* 513, 1 :3–9.

Dirksen, R. T., and K. G. Beam. 1999. Role of calcium permeation in dihydropyridine receptor function. Insights into channel gating and excitation-contraction coupling. *J. Gen. Physiol.* 114:393–403.

Fessenden, J. D., Y. Wang, R. A. Moore, S. R. W. Chen, P. D. Allen, and I. N. Pessah. 2000. Divergent functional properties of ryanodine receptor types 1 and 3 expressed in a myogenic cell line. *Biophys. J.* 79:2509–2525.

Fill, M., and J. Copello. 2002. Ryanodine receptor calcium release channels. *Physiol. Rev.* 82:893–922.

Flucher, B. E., A. Conti, H. Takeshima, and V. Sorrentino. 1999. Type 3 and type 1 ryanodine receptors are localized in triads of the same mammalian skeletal muscle fibers. *J. Cell Biol.* 146:612–629.

Franzini-Armstrong, C., and F. Protasi. 1997. Ryanodine receptors of striated muscles: a complex channel capable of multiple interactions. *Physiol. Rev.* 77:699–729.

Garcia, J., T. Tanabe, and K. G. Beam. 1994. Relationship of calcium transients to calcium currents and charge movements in myotubes expressing skeletal and cardiac dihydropyridine receptors. *J. Gen. Physiol.* 103:125–147.

Grabner, M., R. T. Dirksen, and K. G. Beam. 1999. The II–III loop of the skeletal muscle dihydropyridine receptor is responsible for the bidirectional coupling with the ryanodine receptor. *J. Biol. Chem.* 274:21913–21919.

Gregg, R. G., A. Messing, C. Strube, M. Beurg, R. Moss, M. Behan, M. Sukhareva, S. Haynes, J. A. Powell, R. Coronado, and P. A. Powers.

1996. Absence of the beta subunit (CCHB1) of the skeletal muscle dihydropyridine receptor alters expression of the alpha1 subunit and eliminates excitation-contraction coupling. *Proc. Natl. Acad. Sci. USA.* 93:13961–13966.

Gurnett, C. A., M. De Waard, and K. P. Campbell. 1996. Dual function of the voltage-dependent Ca^{2+} channel alpha 2 delta subunit in current stimulation and subunit interaction. *Neuron.* 16:431–440.

Herrmann-Frank, A., M. Richter, S. Sarkoni, U. Mohr, and F. Lehmann-Horn. 1996. 4-Chloro-m-cresol, a potent and specific activator of the skeletal muscle ryanodine receptor. *Biochim. Biophys. Acta.* 1289:31–40.

Ikemoto, T., S. Komazaki, H. Takeshima, M. Nishi, T. Noda, M. Iino, and M. Endo. 1997. Functional and morphological features of skeletal muscle from mutant mice lacking both type 1 and type 3 ryanodine receptors. *J. Physiol.* 501, 2:305–312.

Kamp, T., M. T. Perez-Garcia, and E. Marban. 1996. Enhancement of ionic current and charge movement by coexpression of calcium channel beta1a subunit with alpha1C subunit in a human embryonic kidney cell line. *J. Physiol.* 492:89–96.

Kim, A. M., and J. L. Vergara. 1998. Fast gating of Ca^{2+} release in frog skeletal muscle revealed by supercharging pulses. *J. Physiol.* 511, 2: 509–518.

McPherson, P. S., and K. P. Campbell. 1993. The ryanodine receptor/Ca^{2+} release channel. *J. Biol. Chem.* 268:13765–13768.

Meissner, G. 1994. Ryanodine receptor/Ca^{2+} release channels and their regulation by endogenous effectors. *Annu. Rev. Physiol.* 56:485–508.

Melzer, W., M. F. Schneider, B. J. Simon, and G. Szucs. 1986. Intramembrane charge movement and calcium release in frog skeletal muscle. *J. Physiol.* 373:481–511.

Murayama, T., and Y. Ogawa. 1997. Characterization of type 3 ryanodine receptor (RyR3) of sarcoplasmic reticulum rabbit skeletal muscles. *J. Biol. Chem.* 272:24030–24037.

Nakai, J., R. T. Dirksen, H. T. Nguyen, I. N. Pessah, K. G. Beam, and P. D. Allen. 1996. Enhanced dihydropyridine receptor channel activity in the presence of ryanodine receptor. *Nature.* 380:72–75.

Nakai, J., T. Ogura, F. Protasi, C. Franzini-Armstrong, P. D. Allen, and K. G. Beam. 1997. Functional nonequality of the cardiac and skeletal ryanodine receptors. *Proc. Natl. Acad. Sci. USA.* 94:1019–1022.

Nakai, J., N. Sekiguchi, T. A. Rando, P. D. Allen, and K. G. Beam. 1998b. Two regions of the ryanodine receptor involved in coupling with L-type Ca^{2+} channels. *J. Biol. Chem.* 273:13403–13406.

Nakai, J., T. Tanabe, T. Konno, B. Adams, and K. G. Beam. 1998a. Localization in the II–III loop of the dihydropyridine receptor of a sequence critical for excitation-contraction coupling. *J. Biol. Chem.* 273:24983–24986.

Neely, A., X. Wei, R. Olcese, L. Birnbaumer, and E. Stefani. 1993. Potentiation of the beta subunit of the ratio of the ionic current to the charge movement in the cardiac calcium channel. *Science.* 262:575–578.

Olcese, R., A. Neely, N. Qin, X. Wei, L. Birnbaumer, and E. Stefani. 1996. Coupling between charge movement and pore opening in vertebrate neuronal alpha1E calcium channels. *J. Physiol.* 497(Pt. 3):675–686.

Perez, C. F., A. Voss, I. N. Pessah, and P. D. Allen. 2003. RyR1/RyR3 chimeras reveal that multiple domains of RyR1 are involved in skeletal-type E-C coupling. *Biophys. J.* 84:2655–2663.

Perez-Reyez, E., and T. Schneider. 1994. Calcium channels: structure, function, and classification. *Drug Dev. Res.* 33:295–318.

Powers, P. A., S. Liu, K. Hogan, and R. G. Gregg. 1992. Skeletal muscle and brain isoforms of a beta subunit of human voltage-dependent calcium channels are encoded by a single gene. *J. Biol. Chem.* 267:22967–22972.

Pragnell, M., M. DeWaard, Y. Mori, T. Tanabe, T. P. Snutch, and K. P. Campbell. 1994. Calcium channel beta-subunit binds to a conserved motif in the I–II cytoplasmic linker of the alpha1-subunit. *Nature.* 368:67–70.

Qin, N., R. Olcese, J. Zhou, O. A. Cabello, L. Birnbaumer, and E. Stefani. 1996. Identification of a second region of the beta subunit involved in regulation of calcium channel inactivation. *Am. J. Physiol. (Cell Physiol.).* 271:C1539–C1545.

Rios, E., and G. Pizarro. 1991. Voltage sensor of excitation-contraction coupling in skeletal muscle. *Physiol. Rev.* 71:849–908.

Rossi, D., I. Simeoni, M. Micheli, M. Bootman, P. Lipp, P.D. Allen, and V. Sorrentino. 2002. RyR1 and RyR3 isoforms provide distinct intracellular Ca^{2+} signals in HEK 293 cells. *J. Cell Sci.* 115:2497–2505.

Sheridan, D. C., W. Cheng, C. A. Ahern, L. Mortenson, D. Alsammarae, P. Vallejo, and R. Coronado. 2003a. Truncation of the carboxyl terminus of the dihydropyridine receptor beta subunit promotes Ca^{2+} dependent excitation contraction coupling in skeletal myotubes. *Biophys. J.* 84: 220–236.

Sheridan, D. C., L. Mortenson, V. Sorrentino, and R. Coronado. 2002. Ca^{2+} induced Ca^{2+} release (CICR) in dyspedic (RyR1 null) skeletal myotubes induced by DHPR beta2a. *Biophys. J.* 82:76a.

Sheridan, D. C., L. Mortenson, V. Sorrentino, and R. Coronado. 2003b. Contribution of ryanodine receptor type 3 to calcium induced calcium release in cultured limb myotubes. *Biophys. J.* 84:108a.

Sonnleitner, A., A. Conti, F. Bertocchini, H. Schindler, and V. Sorrentino. 1998. Functional properties of the ryanodine receptor type 3 (RyR3) Ca^{2+} release channel. *EMBO J.* 17:2790–2798.

Stern, M. D., G. Pizarro, and E. Rios. 1997. Local control model of excitation-contraction coupling. *J. Gen. Physiol.* 110:415–440.

Strube, C., M. M. Beurg, P. A. Powers, R. G. Gregg, and R. Coronado. 1996. Reduced Ca^{2+} current, charge movement, and absence of Ca^{2+} transients in skeletal muscle deficient in dihydropyridine receptor beta1 subunit. *Biophys. J.* 71:2531–2543.

Strube, C., M. Beurg, M. Sukhareva, C. Ahern, J. A. Powell, P. A. Powers, R. G. Gregg, and R. Coronado. 1998. Molecular origin of the Ca^{2+} current of skeletal muscle myotubes selectively deficient in dihydropyridine receptor beta1 subunit. *Biophys. J.* 75:207–217.

Sutko, J. J., and J. A. Airey. 1996. Ryanodine receptor Ca^{2+} release channels: does diversity in form equal diversity in function? *Physiol. Rev.* 76:1027–1071.

Takekura, H., L. Bennett, T. Tanabe, K. G. Beam, and C. Franzini-Armstrong. 1994. Restoration of junctional tetrads in dysgenic myotubes by dihydropyridine receptor cDNA. *Biophys. J.* 67:793–803.

Takeshima, H., T. Ikemoto, M. Nishi, N. Nishiyama, M. Shimuta, Y. Sugitani, J. Kuno, I. Saito, H. Saito, M. Endo, M. Iino, and T. Noda. 1996. Generation and characterization of mutant mice lacking ryanodine receptor type 3. *J. Biol. Chem.* 271:19649–19652.

Takeshima, H., I. Masamitsu, H. Takekura, M. Nishi, J. Kuno, O. Minowa, H. Takano, and T. Noda. 1994. Excitation-contraction uncoupling and muscular degeneration in mice lacking functional skeletal muscle ryanodine-receptor gene. *Nature.* 369:556–559.

Takeshima, H., T. Yamazawa, T. Ikemoto, H. Takekura, M. Nishi, T. Noda, and M. Iino. 1995. Ca^{2+}-induced Ca^{2+} release in myocytes from dyspedic mice lacking the type-1 ryanodine receptor. *EMBO J.* 14: 2999–3006.

Tanabe, T., K. G. Beam, B. A. Adams, T. Niidome, and S. Numa. 1990. Regions of the skeletal muscle dihydropyridine receptor critical for excitation-contraction coupling. *Nature.* 346:567–569.

Tanabe, T., K. G. Beam, J. A. Powell, and S. Numa. 1988. Restoration of excitation-contraction coupling and slow calcium current in dysgenic muscle by dihydropyridine receptor complementary DNA. *Nature.* 336:134–139.

Ward, C. W., M. F. Schneider, D. Castillo, F. Protasi, Y. Wang, S. R. W. Chen, and P. D. Allen. 2000. Expression of ryanodine receptor RyR3 produces Ca^{2+} sparks in dyspedic myotubes. *J. Physiol.* 525:91–103.

Wei, S. K., H. M. Colecraft, C. D. DeMaria, B. Z. Peterson, R. Zhang, T. A. Kohout, T. B. Rogers, and D. T. Yue. 2000. Ca^{2+} channel modulation by recombinant auxiliary beta subunits expressed in young adult heart cells. *Circ. Res.* 86:175–184.

Wilkens, C. M., N. Kasielke, B. E. Flucher, K. G. Beam, and M. Grabner. 2001. Excitation-contraction coupling is unaffected by drastic alteration of the sequence surrounding residues L720–L764 of the alpha 1S II–III loop. *Proc. Natl. Acad. Sci. USA.* 98:5892–5897.

Yamazawa, T., H. Takeshima, T. Sakurai, M. Endo, and M. Iino. 1996. Subtype specificity of the ryanodine receptor for Ca^{2+} signal amplification in excitation-contraction coupling. *EMBO J*. 15:6172–6177.

Yamazawa, T., H. Takeshima, M. Shimuta, and M. Iino. 1997. A region of the ryanodine receptor critical for excitation-contraction coupling in skeletal muscle. *J. Biol. Chem.* 272:8161–8164.

Yang, J., P. T. Ellinor, W. A. Sather, J. F. Zhang, and R. W. Tsien. 1993. Molecular determinants of Ca^{2+} selectivity and ion permeation in L-type Ca^{2+} channels. *Nature*. 366:158–161.

Yang, D., Z. Pan, H. Takeshima, C. Wu, R. Y. Nagaraj, J. Ma, and H. Peng. 2001. RyR3 amplifies RyR1-mediated Ca^{2+}-induced Ca^{2+} release in neonatal mammalian skeletal muscle. *J. Biol. Chem.* 276:40210–40214.